

Temperature Dependent Diffusion Rates of Sulfate in Aquatic Sediments

Will DeRocher, Nathan W. Johnson

Department of Civil Engineering

University of Minnesota Duluth

Submitted to MPCA as a part of the Sulfate Standard Study

12/31/2013

ABSTRACT

Sulfate released to surface waters from natural sources and human activity has the potential to be reduced to sulfide within the anoxic environments of aquatic sediments. This study was conducted to characterize the temperature dependence of sulfate flux and reactions in sediment porewaters through the use of laboratory experimentation and mathematical modeling. Two riverine sediments with contrasting organic carbon content were retrieved from the head and tail waters of the St. Louis River watershed in Northeastern Minnesota, characterized for their bulk geochemistry, and incubated under laboratory conditions to observe the transfer of anions between overlying and sub-surface waters. A simplified numerical model was developed as a part of this study to assist in quantifying time and spatial scales related to sulfate transport in aquatic sediments.

1. Introduction

Context for This Report

This report is one part of a larger study—the Wild Rice Sulfate Standard Study—coordinated by the Minnesota Pollution Control Agency (MPCA) on the effect of elevated sulfate concentrations on wild rice. Minnesota currently has a water quality standard of “10 mg/L sulfate - applicable to water used for production of wild rice during periods when the rice may be susceptible to damage by high sulfate levels.” (Minn. R. 7050.0224, subpart 2). In 2010, the MPCA initiated a multi-year effort to clarify implementation of the state’s wild rice sulfate standard, which had recently come under increased questioning and, contention. Based on a review of available studies and information, the MPCA determined that additional studies were needed to evaluate the effects of sulfate on wild rice before a revision to the numeric sulfate standard could be considered. In 2011 the Minnesota Legislature provided funding to gather this additional information in the Legacy Amendment Bill (Laws of Minnesota, 2011, First Special Session, ch. 6, Art. 2, Sec. 5(j)).

Wild rice is an important aquatic plant in parts of Minnesota, particularly northern Minnesota. It provides food for waterfowl, is also a very important cultural resource to many Minnesotans, and is economically important to those who harvest and market wild rice.

The goal of the overall Wild Rice Sulfate Standard Study (MPCA 2013a) is to enhance understanding of the effects of sulfate on wild rice and to inform a decision as to whether a revision of the wild rice sulfate standard is warranted. The Study consists of several research efforts that have been conducted by several groups of scientists at the University of Minnesota campuses in Duluth and the Twin Cities, under the direction of the MPCA. The data collection phase of the study was completed in December 2013, and is documented in individual reports, along with associated data, from the researchers working on each component of the study.

The primary hypothesis driving the Study has been that if elevated sulfate has a negative effect on the growth of wild rice it is mediated through the formation of hydrogen sulfide in the rooting zone of wild rice, and that elevated iron would mitigate the toxicity of the sulfide by forming insoluble iron sulfide compounds.

The Study components include:

- **Field study of wild rice habitats** to investigate physical and chemical conditions correlated with the presence or absence of wild rice stands, including concentrations of sulfate in surface water and sulfide in the rooting zone.

- **Controlled laboratory hydroponic experiments** to determine the effect of elevated sulfate and sulfide on early stages of wild rice growth and development.
- **Outdoor container experiments utilizing natural sediments** to determine the response of wild rice to a range of sulfate concentrations in the surface water, and associated sulfide in the rooting zone, across the growing season.
- **Collection and analysis of rooting zone depth profiles of dissolved chemicals at wild rice outdoor experiments and field sites** to characterize sulfate, sulfide, and iron in the rooting zone of wild rice.
- **Sediment incubation study** to explore the difference ambient temperature has on the rate that elevated sulfate concentrations in water enter underlying sediment, convert to sulfide, and later release sulfate back into the overlying water.

The MPCA will review the results from individual reports along with existing monitoring data, other relevant scientific studies, pertinent ecological, cultural and historical information, and the original basis for the wild rice sulfate standard to determine if a change to the current wild rice sulfate standard is warranted, and what that change might be. If change(s) are proposed, they would be adopted into Minnesota Rules via the administrative rulemaking process and subject to U.S. EPA approval before the changes could be implemented.

This report focuses on the sediment incubation study conducted at the University of Minnesota Duluth. A mathematical model has been developed along with the sediment incubation results to assist in assessing sediment porewater response to cyclical sulfate loading.

Sulfate is a naturally occurring form of oxidized sulfur that can be transported to surface waters from both natural and anthropogenic sources. Oxidation of sulfide minerals during industrial activity, direct addition during water treatment, burning of sulfur-containing fossil fuels that result in atmospheric deposition of sulfate in the form of acid rain, and decomposition of organic matter, are major sources of sulfate release into the environment (MPCA, 1999). Sulfate readily dissolves into water, making it mobile in lakes, streams, and other surface water systems as well as groundwater. Once released, sulfate can be reduced to sulfide when coupled with bacterial consumption of organic matter. This process occurs only in oxygen-free environments including the hypolimnion of stratified surface waters, water containing high amounts of organics, and aquatic sediment porewaters. Sulfide is thought to be potentially detrimental to the roots and reproduction of certain aquatic vegetation - in particular, wild rice (MPCA, 2011).

This laboratory and modeling study investigated the diffusion of sulfate (SO_4^{-2}) into and out of the anoxic regions of two contrasting freshwater aquatic sediments under warm and cold temperatures. Two characteristically different sediments - high organic and low organic - were retrieved from local streams and incubated at two temperatures - 4.5 °C and 23 °C - for nine months. The aerated and mixed overlying water was spiked with sulfate and tracer ions and carefully monitored throughout the duration of the experiment to record the flux into the sediment from the overlying water. Over that period, small volume samples were periodically extracted from the porewaters of the microcosms and analyzed to help determine rates of diffusion. In addition to physical modeling of sulfate diffusion, a mathematical model that describes the movement of sulfate between surface waters and sediment was also developed. The model describes the temperature dependence of sulfate diffusional flux and reactions in sediments.

The goal of this study is to be able to answer the questions: how quickly does sulfate diffuse into sediment porewaters? How much sulfate is consumed by the bacteria within the sediment at a given time and temperature? How long does it take for the sulfate to diffuse back out of the sediment after the surface water concentration has diminished? Rates and timescales of sulfate transport and reaction elucidated by the physical and mathematical models used for this study can be used as a tool to assist policy makers in their efforts to effectively manage sulfate discharges in order to provide protection of wild rice and accommodate responsible anthropogenic activities within the state.

2. Materials and Methods

Experimental setting & materials

Experimental sediments were retrieved from two locations within the St. Louis River watershed. The Partridge River (PR) sampling location is near the headwaters of the St. Louis River on the East-central portion of the Mesabi Iron Range in Northern Minnesota (Figure 1, Table 1). The Partridge River site provided high organic sediment from a slow-moving part of a sulfate-impacted river where wild rice had been observed in recent years. The second sampling location, North Bay (NB), is near the tail waters of the St. Louis River, approximately 15 km upstream from the entrance into Lake Superior in the St. Louis River Estuary. The North Bay site, a protected bay away from the main channel, provided a lower organic sediment from a location where rice had also been observed in recent years. In January 2013, approximately 50 L of sediment was recovered from the top 10 cm of the river beds, transported back to the University of Minnesota – Duluth, and homogenized.



Figure 1 Sediment Retrieval Sites, Northern site- Partridge River, organic sediment in upper sub-watershed of St. Louis River; Southern site-North Bay, low organic sediment, St. Louis River Estuary

Table 1 Characteristics of sites where experimental sediments were retrieved

	Latitude	Longitude	Overlying SO ₄ ^{-2,a}	In-situ Porosity ^b	Carbon Content
Partridge River	47° 31.271'	-92° 11.410'	43.9 mg/L	91%	Awaiting lab results
North Bay	46° 39.188'	-92° 14.225'	15.3 mg/L	74%	Awaiting lab results

^a Site average at time of sediment collection; ^b 0-10 cm avg.

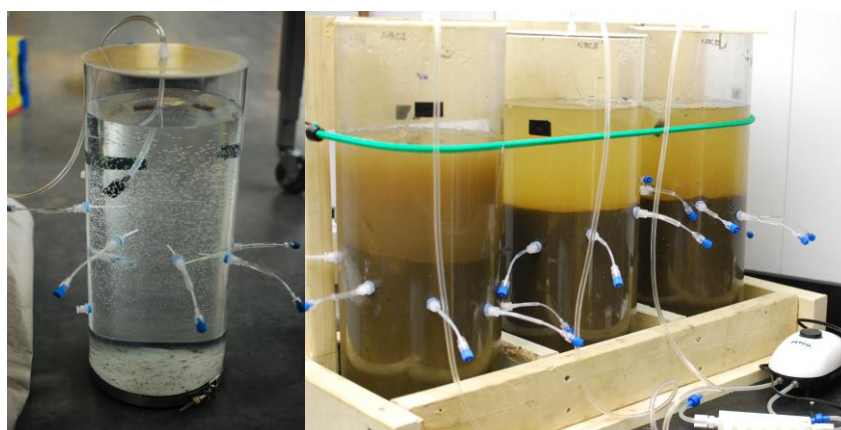
Experimental Setup

Microcosms consisted of polycarbonate plastic tubing (20 cm ID, 0.05 cm wall thickness) with a sealed bottom and Rhizon® soil moisture samplers fixed and sealed at varying depths along microcosm's profile to extract water from the pore space of the sediment, (Seeberg-Elverfeldt et al., 2005). The Rhizon® samplers were used to take 3mL samples of porewater at specific time points throughout the experiment for the monitoring of anion transport within the sediment (Figure 2b). Homogenized sediment was transferred to microcosm tubes, and gently consolidated by the use of a vibration table to minimize settling during the experiment. Fresh site water was placed over the sediment and the microcosms and allowed to equilibrate to lab conditions for three weeks prior to the beginning of experiments.

Microcosms were loosely capped with an acrylic plate to avoid evaporative losses. An aeration system was also included to provide oxygen and mixing to the overlying water. Air for the bubbler system was pumped through an activated carbon filter to remove any airborne contaminants, then through a HEPA filter to remove any particulate matter, and finally through a sealed flask of deionized water to hydrate the air, to avoid evaporative losses (Figure 2a). The microcosms were incubated in dark, temperature-controlled conditions throughout the experiment to minimize disturbances and to eliminate variables such as photosynthesis (Figure 2c). Triplicate microcosms were constructed for each temperature. Three microcosms filled with North Bay Sediment were incubated at 4.5 °C for the duration of the experiment and three identical microcosms were incubated at 23 °C . An analogous set of microcosms were constructed and incubated using sediment from the Partridge River.



(a)



(b)

(c)

Figure 2 Experimental microcosm setup. (a) Air pump, activated carbon filter, HEPA filter, and sealed flask of deionized water and manifold delivering air to microcosms (b) Test microcosm filled with water prior to addition of sediment. Rhizon® filters are positioned in a helical pattern around the circumference of the polycarbonate tube (8 cm horizontal, 2 cm vertical separation) to reduce the influence of one filter on the neighboring filters (c) Microcosm test setup

Experimental treatments

The experimental portion of the study occurred in three phases to analyze the flux of sulfate and several inert, tracer anions across the sediment-water interface. Water overlaying the sediment in each microcosm was continuously mixed and aerated to eliminate chemical gradients near the sediment-water interface in an effort to mimic conditions in a shallow natural stream that might receive sulfate-enriched

discharges. After an initial three-week equilibration period, Phase I began with a chloride spike (30 mg/L) into the surface water of the all of the microcosms. Elevated chloride concentration was maintained by adding aliquots of concentrated sodium chloride stock solution intermittently until the start of the next phase (Table 2, Appendix A, Table 1). During Phase I, the sulfate concentration in the overlying water was also monitored weekly, and was replaced when necessary to maintain concentrations similar to those experienced in the field.

Table 2 Sulfate and tracer manipulations during experimental phases.

Experimental Phase	Overlying water Sulfate Amendment	Overlying water Tracer Amendment	Length
Equilibration	None	None	3 weeks
Phase I	None	Chloride (~30 mg/L)	6 weeks
Phase II	~ 300 mg/L	Fluoride (~16 mg/L)	11 weeks
Phase III	None	Bromide (~20 mg/L)	8 weeks

Phase II, the sulfate loading phase, was initiated by replacing the overlying water with fresh site water spiked with both sodium sulfate (approximately 300 mg/L as sulfate) and sodium fluoride (16 mg/L as fluoride) and no chloride (Table 2). Sulfate was spiked at the outset of Phase II and re-spiked three times throughout the 11 week loading phase. The 300 mg/L target concentration was chosen since several streams contributing to the main stem of the St. Louis River regularly see such sulfate concentrations during various seasons. Sulfate amendments occurred only periodically to enable the quantification of flux into sediment through weekly surface water measurements. During Phase II, chloride diffused out of the porewaters into the surface waters. However, porewater samples were preserved with hydrochloric acid and therefore chloride concentrations could not be quantified accurately during the subsequent phases. The sulfate and fluoride spikes to surface water induced a sharp sulfate gradient between the surface and porewaters, providing the driving force for diffusional flux.

Phase III, the recovery phase, was initiated by replacing the overlying water with fresh site water spiked with sodium bromide (20 mg/L as bromide; no additional chloride, sulfate, or fluoride) which was maintained for 9 weeks. The sulfate recovery phase was designed to simulate the end of sulfate-elevated discharge to surface waters, with the goal of determining how long sediment in a river system may be exposed to residual sulfate, even after sulfate concentrations in the overlying water are reduced. In between each phase, a three-day interlude in which clean, unamended site water occurred before starting the next phase.

To maintain target experimental conditions, surface water samples were collected and analyzed weekly from all replicate microcosms. The overlying water was changed as often as necessary to maintain the ion concentration gradient between the sediment and the water or as otherwise deemed necessary (i.e. due to significant conductivity or pH changes, or obvious clouding of the water)(Appendix A, Table 1). The amended overlying water used during incubations was retrieved from the same locations where the sediments were obtained.

Sampling Methods

At the outset of the experiments, *in situ* conditions and initial laboratory microcosm conditions were characterized to be able to evaluate how closely the laboratory setup mimicked field conditions. While retrieving the bulk sediment for microcosms, 7 cm diameter polycarbonate cores were collected, transported to the lab, and sectioned into 1-2 cm depth intervals for the analysis of *in situ* porosity, acid volatile sulfide (AVS), and organic content. At the beginning of the experiment, two additional microcosms were set up and maintained until the end of Phase I at which time similar stratigraphic analysis was conducted. At the end of the experiment, all laboratory microcosms were deconstructed and similar stratigraphic analysis was conducted. In addition to chemical characterization, samples were taken from microcosm materials to measure the quantity and types of macro organisms in the sediment. Sampling was conducted in accordance with the Wild Rice Sulfate Standard Quality Assurance Plan (MPCA, 2013b)

Throughout the experimental phases, samples from the overlying water and porewater were collected in order to characterize the physical and chemical processes controlling sulfate transport and transformation as well as aid in making decisions about proceeding through the experiment. Basic measurements of the overlying water including water depth, temperature, conductivity, pH and dissolved oxygen were made twice a week using a measuring tape and calibrated Hydro-Lab Sonde to ensure consistent, oxygenated conditions throughout the test. Anion samples (10 mL) were collected, filtered through 0.45 μm polyethersulfone (PES) filter, and quantified weekly in order to monitor the flux of sulfate both into and out of the sediment and maintain the concentration of the tracer ions within the surface water.

Porewater samples were taken 1-2 times during each experimental phase to monitor the concentration of sulfate and tracers as well as sulfide, iron, and pH within the pore fluids. A more in-depth porewater analysis including pH, iron, sulfide, and ion concentration was conducted at the beginning of the

experiment and at the end of each phase. Porewater samples for anion concentrations only were collected more frequently to support model simulations and define sulfate concentrations in pore fluids.

Analytical methods

Dissolved ferrous iron (Fe^{2+}) was quantified in porewater samples using the phenanthroline method (Eaton et al. 2005). Reagents were preloaded into vials to preserve the sample and prepare it for analysis using spectrophotometry. Porewater sulfide concentrations were analyzed using the Hach 8131 method, an adaptation of method 4500-S²-D in Eaton et al. (2005). Anion concentrations for the surface waters (0.45 μm PES filter) and porewaters (0.2 μm Rhizon® filter) were quantified following filtration using ion chromatography, method 4110 C (Eaton et al., 2005) with chemical suppression of eluent conductivity on a Dionex ion chromatograph using the Chromelion software for peak integration.

For high-resolution solid phase samples from the *in situ* and laboratory cores, ASTM D2216-10: Standard Methods for Laboratory determination of water (moisture Content of Soil and Rock by mass method) as well as ASTM D 854-10: Standard test for specific gravity of soil solids by water in a volumetric flask were used to quantify the moisture content and specific weight of the of the sediment solids. Results from both tests were used to calculate sediment porosity as a function of depth in the sediments.

AVS, total carbon, and sulfide data for *in situ* sediments and laboratory microcosms are not yet available from samples submitted for analysis. These results will be included in subsequent versions of this report as they become available.

Modeling Methods

Numerical model of tracer ion diffusion

The model presented here for the tracer anions accounts for diffusional flux and differential sediment porosity and tortuosity (Boudreau, 2003) as a function of depth, and neglects reactions within the sediment. This assumption is warranted as chloride, fluoride, and bromide are inert and stable under both oxidizing and reducing conditions and interact minimally with the solid phase. The water-only diffusional coefficients for the different experimental anions were adjusted for temperature and porosity in the model calculations (Appendix B, Table 1). A thorough description of the mathematical steps taken to develop the model is given in Appendix B.

Sediment porosities were calculated based on the measured moisture content from composited depth profile samples and specific gravity of the corresponding sediments (Appendix B). Modeled results

are displayed for the same time point as the samples were taken from the porewater (to within 24 hours). The numerical model utilizes 0.25 cm depth increments and 30-minute time steps with a constant concentration as the upper boundary, and initial conditions similar to what was observed in the microcosms.

Reactive transport model for sulfate

The effective diffusion coefficients for bromide that matched experimental observations in warm and cold microcosm porewaters (Appendix B, Table 1) were adjusted for molecular properties to obtain effective diffusion coefficients for sulfate in warm and cold temperatures. For the preliminary model, an effective first order reaction rate for sulfate (0.15 / day) was constrained by the observed sulfate penetration depth into sediment porewaters of the warm microcosms during Phase II. The effective first order reaction rate was adjusted for temperature based on slightly deeper sulfate penetration in cold microcosms during Phase II. The first order rate at 4 °C was 0.040 /day, which amounts to a Q_{10} of 2.0, slightly lower than the average temperature dependence reported in Pallud and VanCappelen (2006) for sulfate reduction in surficial freshwater sediment ($Q_{10} = 2.25 - 2.9$).

Despite having apparently quite different organic matter contents (awaiting results from laboratory analysis at time of this report), no large differences were observed between the rate or depth of sulfate penetration between Partridge River (PR) and North Bay (NB) sediment during Phase II. Additionally, the rate of tracer ion diffusion was not clearly different between the sediments (Figures 4-6). For these reasons, a single sulfate reduction rate and a single temperature-dependent effective diffusion rate was used for sulfate simulation of both systems. However, separate simulations were necessary for the warm and cold conditions since the warm Partridge River microcosms contained a higher upper sulfate boundary condition (Figure 4) and the cold Partridge River microcosms contained a non-zero initial condition (Appendix A, Figure 1). The equations, boundary, and initial conditions describing sulfate diffusion and reaction simulations are included in Appendix C.

3. Results

Equilibration Phase I

Over the six-week Phase I, consistent with experimental objectives, overlying water observations showed that chloride concentrations remained consistently elevated in the overlying water of both warm and cold microcosms, thereby providing an elevated upper boundary condition to characterize diffusion into sediment porewaters (30-45 mg/L for Partridge River and 20-30 mg/L for North Bay) (Figure 2a and

2b). Sulfate in the overlying water remained constant at about 100 mg/L in Partridge River microcosms and was typically between 30 and 40 mg/L in North Bay microcosms. During the equilibration time before chloride was added to begin Phase I, it was noted that the sulfate concentration progressively increased within the surface water of the Partridge River microcosms, most likely due to the oxidation and solubilization of sulfur within the sediment as a result of disturbances the sediment underwent in going from field to laboratory settings (Appendix A, Figure 3).

Due to uncertainty in the exact vertical position of porewater sampling locations relative to one another and to the sediment-water interface, the average of observed values for tracer concentrations at the location defined as zero depth was used as an upper boundary condition for modeling tracers. Modeled results were compared to porewater observations which reflect average values for sample depths in close proximity (0.5 cm maximum) as measured from the sediment water interface. Standard deviation bars are given for each point where more than one value was averaged.

Chloride was uniformly present between 5 and 10 mg/L in microcosm porewaters at the initiation of Phase I and, consistent with modeling results after four days, chloride concentration notably increased within the sediment porewaters to a depth of 1 cm in the North Bay sediments and 3 cm within the Partridge River sediments (Figure 2 panel c and d). Sulfate concentrations were uniformly low in sediment porewaters during Phase I except in the top 3-5 cm where sulfate was assumedly being transported from the overlying water and in the 0-10 cm cold Partridge River porewaters (Appendix A, Figure 1). A possible explanation for this latter observation is that residual sulfate from the oxidation of sulfide minerals during microcosm construction likely elevated sulfate in Partridge River porewaters. Reduced biological rates of sulfate reduction in the cold incubated microcosms likely allowed the sulfate to persist.

The nearly uniform decrease in porewater sulfate from ~200 mg/L to ~100 mg/L over a 4 week period prior to the initiation of Phase I in cold Partridge River microcosms (Appendix A, Figure 1a and 1b) suggests a sulfate reduction rate of approximately $3.5 \text{ mg L}^{-1}\text{day}^{-1}$ or approximately $37 \text{ } \mu\text{mol L}^{-1}\text{day}^{-1}$ which is consistent with maximum rates reported by Pallud and Van Cappellen (2005) for freshwater sediment at depths below 5 cm at 21° C ($10\text{-}100 \text{ mg L}^{-1} \text{ day}^{-1}$) and temperature adjustments of 2-4 times slower per 10 °C drop in temperature, as suggested by Fossing et al. (2001) and Pallud and Van Cappellen (2005).

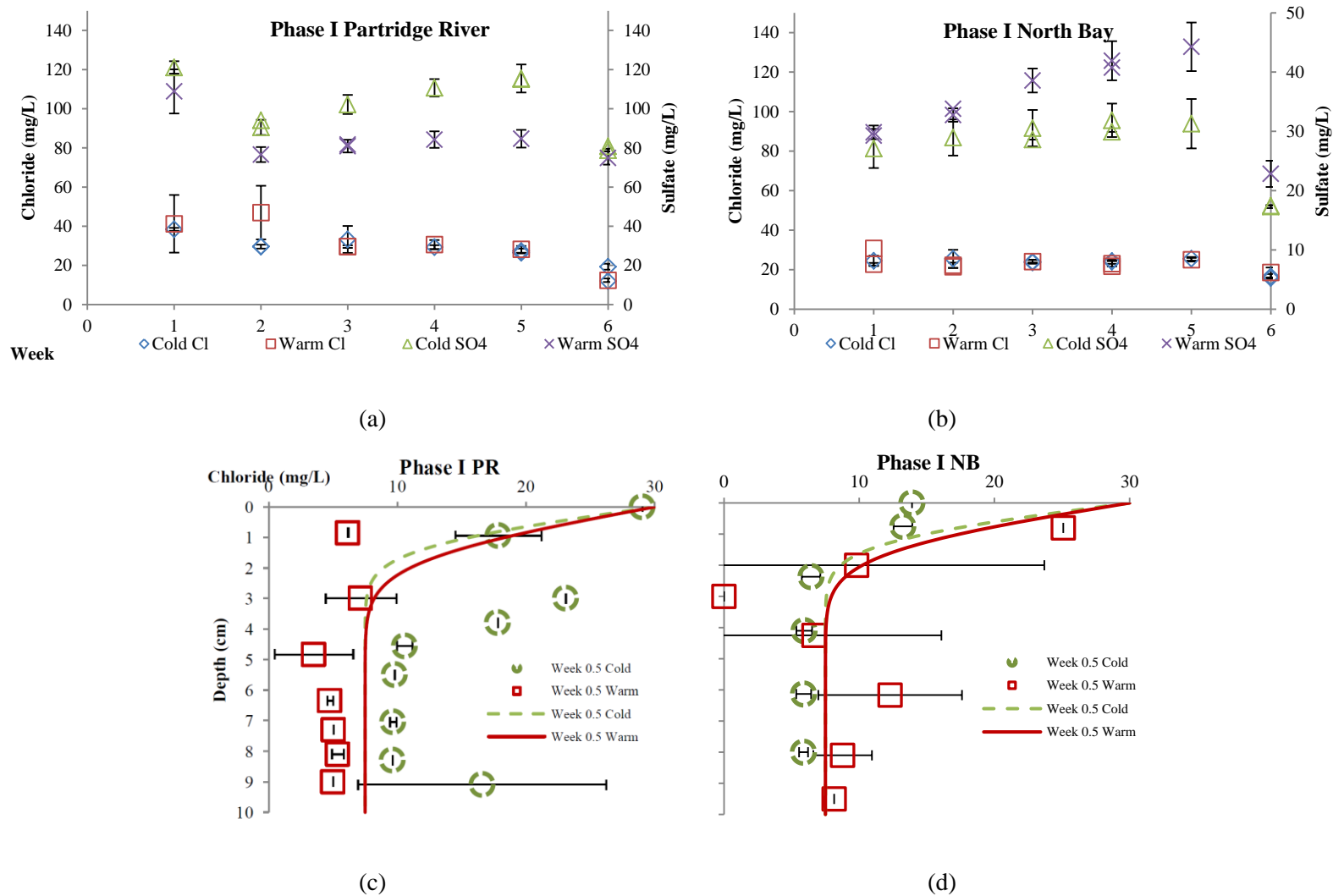


Figure 3 Phase I overlying water and porewater anion concentrations in warm and cold microcosms (a) Partridge River sulfate and chloride in overlying water (b) North Bay sulfate and chloride in overlying water (c) Partridge River porewater chloride observations (symbols) and model (lines) (d) North Bay porewater chloride observations (symbols) and model (lines).

Table 3 Phase I average anion concentrations for surface water in experimental microcosms

	4.5°C	23°C
	(mg/L)	(mg/L)
Partridge River chloride	27.3	31.3
North Bay chloride	21.5	21.7
Partridge River sulfate	101.0	84.6
North Bay sulfate	27.0	34.1

Loading Phase II

Phase II was an eleven-week period during which sulfate and fluoride were spiked into the surface water (avg. 270-280 mg/L and avg. 10-15 mg/L respectively, Figure 4). Initial fluoride concentrations within the porewaters ranged from 0.3-0.6 mg/L, well below spike levels. Porewater sulfate concentrations were generally less than 25 mg/L at the outset of Phase II in both. The only exception to this is the cold Partridge River porewater, which had approximately 100 mg/L in porewater as a residual from the equilibration phase; and surface (<3 cm) sediment, which was likely elevated due to transport from the overlying water. Spiked levels of sulfate were set at ~200 mg/L, well above the initial concentration range seen the porewaters, which effectively established a well-defined gradient between the surface waters and porewaters. Fluoride provided an inert anion tracer that could be measured in parallel with sulfate. Fluoride was spiked initially and periodically re-spiked (Appendix B, Table 1) throughout Phase II to keep an average fluoride concentration between 10 and 15 mg/L in the surface water.

Prior to beginning Phase II, average sulfate concentrations in the surface water remained between 25 and 100 mg/L (Table 3). Similarly to the equilibration period (Appendix A, Figure 3), sulfate concentrations began to progressively rise in the Partridge River warm microcosm surface water about halfway through Phase II (Figure 4, panel a, weeks 4-11). Sulfate concentrations in excess of 650 mg/L were observed in the 23°C Partridge River microcosms near the end of Phase II, while the highest concentration in the other microcosms ranged from 350-365 mg/L. This same increase occurred in all three replicates of the warm Partridge River sediments, suggesting it was not an anomalous occurrence. The most likely cause for these unexpected high sulfate concentrations lies in bioturbation by naturally occurring organisms within the sediment, oxidizing the available iron sulfide. As the sulfur became oxidized, it was readily transported in the water, increasing porewater concentrations until the gradient between the porewaters and surface waters was reversed, causing a net flux of sulfate out of the sediment.

Because the fluoride spike was significantly higher than the background levels within the porewaters, modeled diffusional mass transport from the surface water predicted that porewater concentrations of fluoride would increase, which corresponds well to experimental observations. Within a week, porewater fluoride concentrations of the Partridge River sediments at a depth of 0.5 cm were a quarter of surface water concentrations. Within 6 weeks, porewater fluoride concentrations of the warm Partridge River sediments at a depth of 1.0 cm were a quarter of the surface water concentration and the cold porewater concentrations were slightly lower. By 9 weeks after the initial spike, porewater fluoride concentrations of the warm Partridge River sediments at a depth of 2.0 cm were a quarter of the surface water concentration, and again the cold treatments were slightly lower (Fig. 4c). Analysis of the North Bay porewater data revealed nearly twice the concentration of fluoride at the same time points. The temperature dependence of porewater concentrations predicted by the model was consistent with observations, showing concentrations in the cold microcosm just slightly lower (Fig. 4d). Diffusion of fluoride was adjusted in model simulations to match observations; however, effective diffusion for warm and cold conditions were roughly 65 % slower than expected based on porosity- and temperature-adjusted values. This difference is likely due to the modeled assumption of a constant upper boundary condition which was clearly not present for fluoride during the initial 6 weeks of Phase II (Fig. 4a,b). Consequently, the calibrated effective diffusion coefficients for bromide in Phase III were used to make estimates for effective sulfate diffusion.

Sulfate Loading

Due to the unforeseen rise in overlying sulfate concentrations in the Partridge River warm microcosms, the temperature-dependence of porewater sulfate concentrations during the end of the loading phase and recovery phase was difficult to distinguish. Sulfate in sediment porewaters throughout Phase II and Phase III were normalized to the surface water sulfate concentration for the preceding week (Figure 5). By normalizing the porewater to contemporaneous surface water concentrations, temperature-related differences in the depth of sulfate penetration and concentration comparisons could be made more readily. Surface water sulfate concentrations used for normalization and raw porewater sulfate concentrations (not normalized) are included as (Appendix A, Table 2 and Appendix A, Figure 2).

Normalized sulfate levels in the porewaters increased between 0 and 6 weeks of Phase II; however changes in porewater concentration between the 6th week and 9th week were minimal in both North Bay and Partridge River sediments, indicating steady state concentrations had been reached. Almost immediately upon beginning Phase III, the concentration in the upper portion of the sediment dropped back to match the surface water sulfate level. The concentrations at lower depths respond more

slowly, but by the 16th week matched surface water levels due to diffusion back out of the sediment and sulfate reduction within the soil.

Sulfate has a diffusional coefficient nearly half that of bromide but reaches detectable concentrations at greater depths much more quickly. This difference is in part due to the difference in concentration gradients between sulfate and bromide, and the difference in molecular weight. Surface water sulfate was approximately 275 mg/L higher than the porewater concentrations, whereas there was only a 17 mg/L difference for bromide. By the end of Phase II, depths of 4 cm in the Partridge River sediment and 3 cm in the North Bay sediment were exposed to half of the spiked concentration.

Within twelve weeks of the sulfate spike to overlying water, sulfide concentrations had slightly increased in the porewaters of North Bay cold microcosms (2 μM at 4-6 cm below the sediment water interface) and Partridge River warm microcosms (1.3 μM at 3 cm below the surface, however this is near the 0.7 μM reporting limit of the Hach method used for analysis) (Figs. 10b, 14b).

Over the course of Phase II, the concentration of sulfate in the surface water followed a downward trend in three of the four test treatments (the overlying water sulfate concentration in the warm Partridge River microcosms increased for reasons previously discussed). A summation of the concentration drops per unit area provides the total mass lost to the porewaters due to flux over the first 4 weeks of Phase II (Table 4). It is evident when comparing the warm and cold sediments that more mass fluxed into the warm sediments than the cold sediments, even though this is not immediately apparent from the porewater sulfate sampling that was conducted (Figure 5). The difference between the sulfate mass that fluxed into the sediment and what was evident in the porewaters is most likely due to biological consumption.

Table 4 Mass loss of sulfate and fluoride from surface waters to the porewaters of experimental microcosms over the first 4 weeks of Phase II

	Partridge River Cold (mg/cm²)	Partridge River Warm (mg/cm²)	North Bay Cold(mg/cm²)	North Bay Warm (mg/cm²)
Sulfate	0.6	0.7	1.5	2.3
Fluoride	0.3	0.4	0.2	0.4

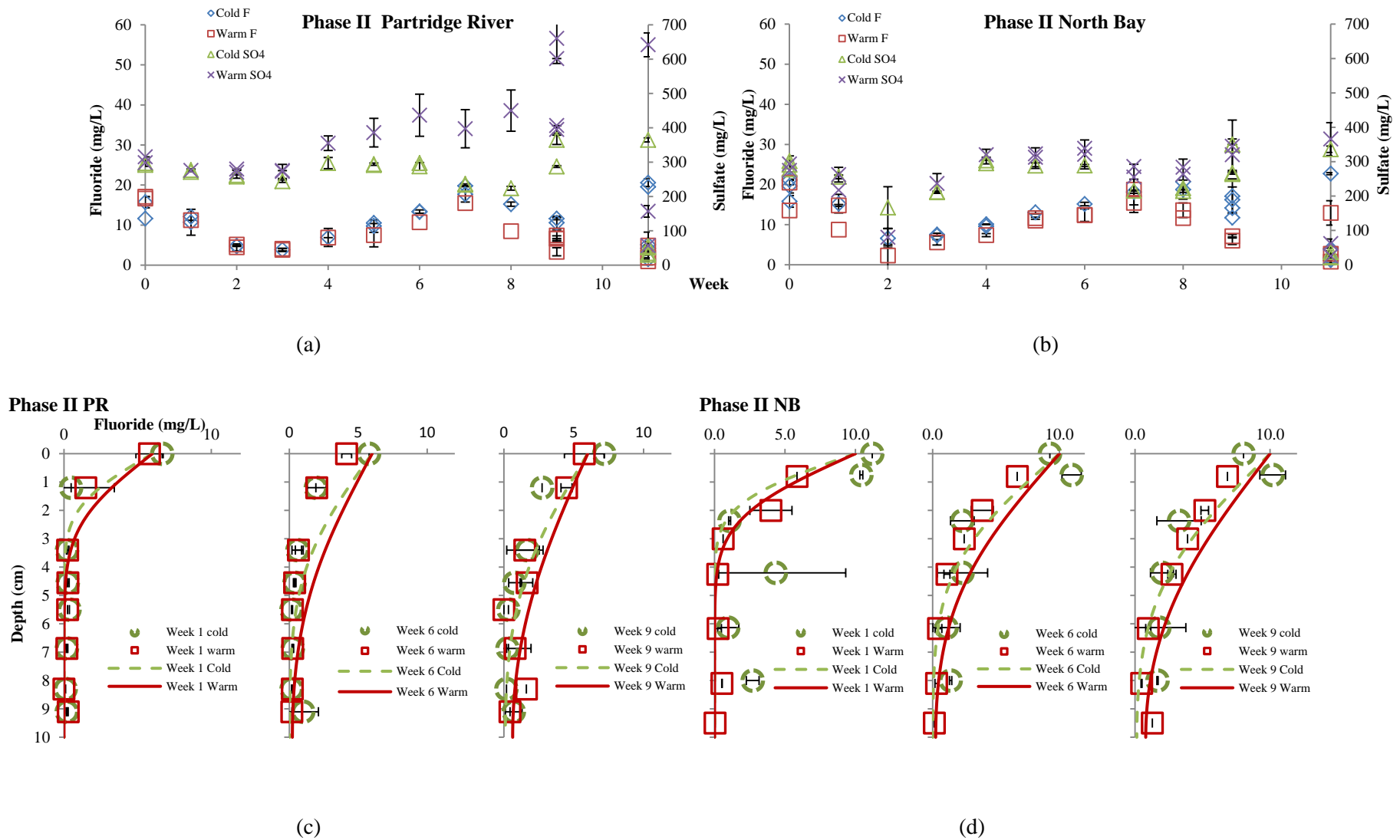


Figure 4 Phase II overlying water and porewater chemistry in warm and cold microcosms (a) Partridge River sulfate and fluoride in overlying water (b) North Bay sulfate and fluoride in overlying water (c) Partridge River porewater chloride observations (symbols) and model (lines) (d) North Bay porewater fluoride observations (symbols) and model (lines).

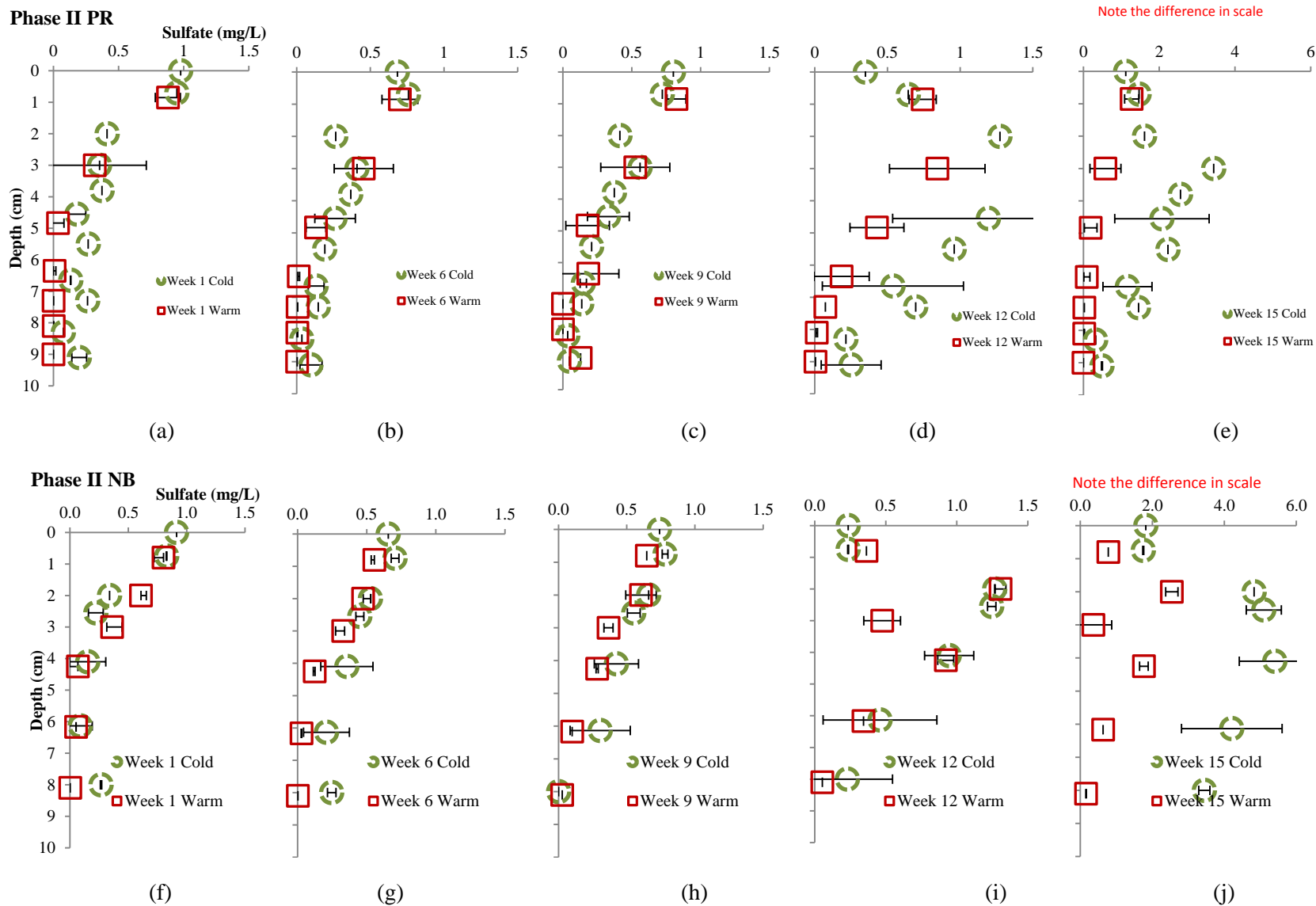


Figure 5 Porewater sulfate concentrations in microcosms during Phase I and Phase II. Times denote weeks from the initiation of Phase II (sulfate spike) and scales are porewater concentration as a percentage of surface water concentration for the preceding week. (a-e) Partridge River warm and cold porewater sulfate. (f-j) North Bay warm and cold porewater sulfate. Values denote the average of measurements from replicate microcosms at the specified depth. Horizontal error bars denote the standard deviation of three replicate microcosms. Sulfate concentrations in panels e and j have a different scale as the surface water concentration was dropped back to ambient levels and porewater concentrations remained high from the previous phase.

Table 5 Phase II average anion concentrations for surface water in experimental microcosms

	4.5°C (mg/L)	23°C (mg/L)
Partridge River sulfate	282.2	395.2
North Bay sulfate	268.9	283.2
Partridge River fluoride	12.2	8.3
North Bay fluoride	14.8	11.4

Recovery Phase III

At the beginning of Phase III, the surface water sulfate concentration was lowered to ambient concentrations (approximately 11 mg/L and approximately 20 mg/L for North Bay and Partridge River respectively) using water retrieved from the sites. The outward flux of sulfate from the sediment was monitored during Phase III, along with the inward flux of bromide. During this phase, the high concentration of sulfate within the porewaters diffused back into the surface waters. The surface water was replaced weekly to maintain an upward gradient in sulfate concentration, similar to field conditions where low sulfate water in a river would be typical during spring flows due to snow melt and potential sulfate loading cutoffs.

Initial bromide concentrations ranged from 0-2 mg/L within the porewaters prior to Phase III. Within the first week of spiking bromide into the surface waters, concentrations nearly half that of the surface waters had penetrated 0.5 cm into the sediments of both Partridge River and North Bay. Throughout Phase III, both the North Bay and Partridge River depth profiles for bromide looked very similar; by three weeks half the surface concentration was measured at depths of 3 cm in Partridge River cold, 4 cm in North Bay cold, 5 cm in Partridge River warm and 5 cm in North Bay warm. By seven weeks, bromide at half the concentration of the surface water was observed at 7 cm in Partridge River warm, 4 cm in Partridge River cold, 6 cm in North Bay warm and 4 cm in North Bay cold.

Sulfate flux out of the sediment occurred rapidly over the first week of the surface water being replaced with fresh site water during Phase III, the recovery phase. After two overlying water replacements within one week, sulfate levels remained steady at 30-40 mg/L in all of the microcosms except the warm Partridge River trials, in which overlying water sulfate continued to rise. With frequent water replacement, the warm Partridge River overlying sulfate concentrations dropped from 300 to 150 mg/L SO_4^- over the course of three weeks and slowly dropped to 40 mg/L over the course of the next 5 weeks. Sulfate concentrations were lowered in the surface water by replacing the overlying water with water retrieved from the site. Sulfate concentrations in this water rose due to the outward flux of sulfate

from the sediment. The porewater concentrations of sulfate within all of the microcosms reacted to the upper boundary condition. Sulfate quickly diffused out of the upper two centimeters of sediment and slowly diffused out or was consumed in deeper regions of the sediment (Fig. 5d,e). Three weeks after the surface water concentration was dropped from 300 mg/L to 15 mg/L, the sulfate levels of the first two centimeters of sediment nearly matched the surface water concentration.

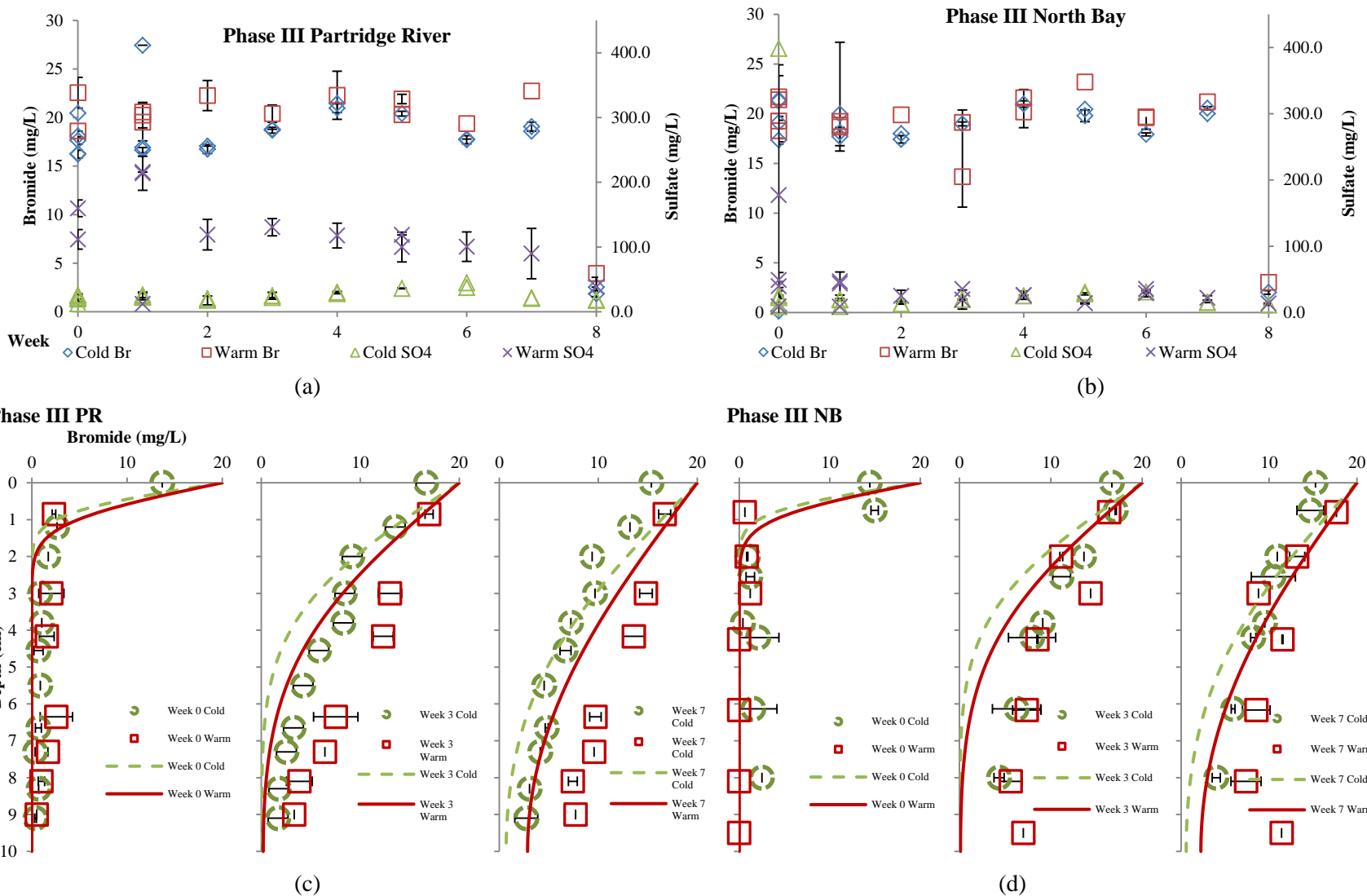


Figure 6 Overlying water and porewater chemistry in warm and cold microcosms (a) Partridge River sulfate and bromide in overlying water (b) North Bay sulfate and bromide in overlying water (c) Partridge River porewater bromide observations (symbols) and model (lines) (d) North Bay porewater bromide observations (symbols) and model (lines).

Table 6 Phase III average anion concentrations for surface water in experimental microcosms

	4.5°C (mg/L)	23°C (mg/L)
Partridge River sulfate	27.4	116.1
North Bay sulfate	37.9	37.3
Partridge River bromide	17.2	18.2
North Bay bromide	17.3	18.7

Experimental and *in situ* sediment and porewater characteristics

The characterization of sediment conditions conducted at the end of each experimental phase provides a means of comparing laboratory measurements to field conditions. Sediment porosity was calculated from the measured specific gravity of the respective soils and the moisture content (wet basis). The difference in porosity between *in situ* (avg. 91% PR, avg. 74% NB) and laboratory settings (avg. 80% PR, avg. 73% NB) is most likely due to sediment homogenization and consolidation at the beginning of the experiment. The top ten centimeters of sediment was collected from the site and homogenized in the laboratory. Variation in porosity between the experimental microcosms at the end of Phase I and Phase III was minor (+/- 4%) and would not significantly alter the experimental results. (Figures 7a-c, 11a-c). The difference in porosity between Partridge River and North Bay sediments was more substantial and the difference can be attributed to the makeup of the sediments. Partridge River sediment had a higher organic content and was less dense ($\rho_s = 2.60$), the North Bay sediment was more silt-like and more dense ($\rho_s = 2.62$). Specific gravity is the relationship between the sediment density and water's density. Porosity depends upon the specific gravity of the sediment as well as the moisture content of the sediment. A 0.02 difference in specific gravity is compounded within the porosity calculations (Appendix B). The higher porosity in the Partridge River sediment would allow quicker penetration of sulfate but also a quicker recovery than the North Bay sediment, once the surface water concentration had decreased. (Figure 5e, 5j) The North Bay sediment has lower porosity, effectively restricting the movement of anions in solution. Sulfate trapped in the porewaters has a greater potential to be reduced to sulfide.

pH measured during experiments differed little from in-situ condition and varied only slightly throughout the experiment, most noticeably within the warm microcosms (Cold microcosms approximately 7.1 and, warm microcosms 6.9). Differences between warm and cold porewater pH may be reflective of the biological processes taking place within the sediment, since organisms are likely less active within the cold microcosms (similar to *in situ* conditions, pH approximately 7.1). (Figures 8 and 12)

The dissolved iron (II) concentrations measured during experiments deviated significantly from *in situ* conditions for both Partridge River (78% increase over the course of the experiment, avg. 526 $\mu\text{mol L}^{-1}$ -*in situ*, avg. 937 $\mu\text{mol L}^{-1}$ – end Phase III) and North Bay (600% increase over the course of the experiment, avg. 32 $\mu\text{mol L}^{-1}$ -*in situ*, avg. 226 $\mu\text{mol L}^{-1}$ – end Phase III) (Figures 9, 13) The differences between *in situ* and laboratory porewater iron(II) concentrations may be partly due to the disruption, collection, transportation, and homogenization the sediment underwent; but this difference could also be caused by the high anion concentrations or oxygen introduced within the anoxic regions of the porewaters. The solubility of iron is affected by pH, oxidation potential, salinity, and the concentration of complexing ions (Fairbrother and Wentzel, 2007). Anions (chloride, fluoride, and, sulfate) complex with iron, potentially mobilizing it from loosely bound solid phases into a dissolved phase. These ligands are inert with respect to sulfate, but can influence the iron. Ionic complexation within the sediment porewaters could explain the increased iron (II) concentrations observed throughout the course of the experiment. Alternatively, reduced iron phases oxidized during experimental manipulations may have been reduced again, leading to the accumulation of the more mobile ferrous iron in pore fluids. Either of these processes, or some combination of the two, provide an explanation of the noted increase in dissolved ferrous iron throughout the experiment.

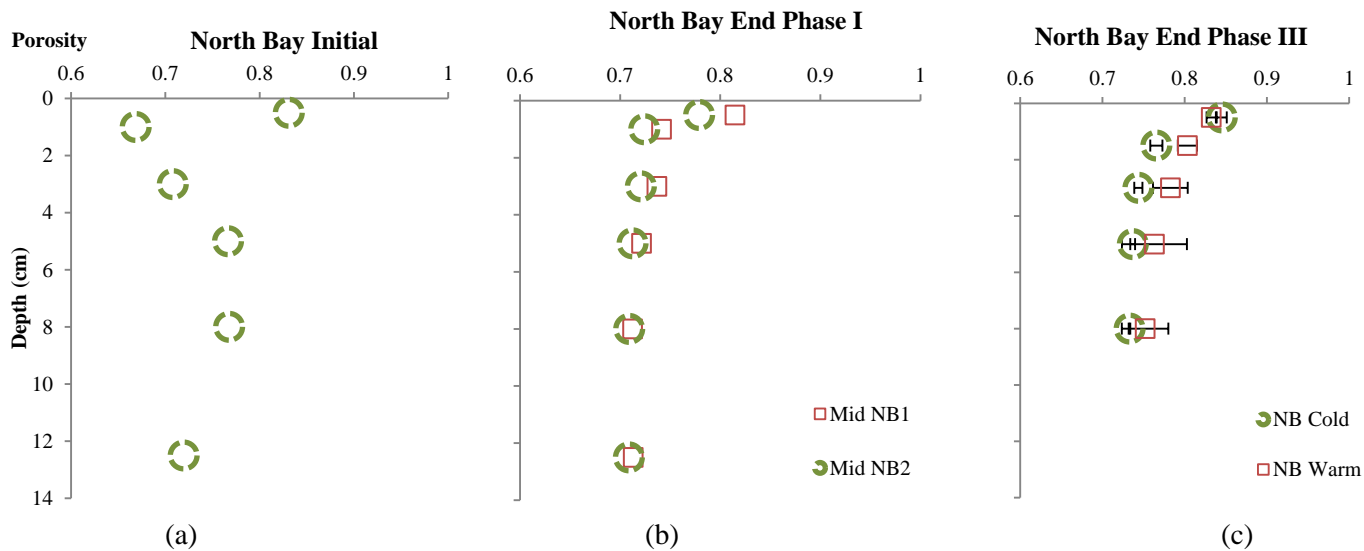


Figure 7 Porosity measurements based on moisture content depth profile of North Bay sediments, (a) *in situ* conditions, (b) mid way through experiment, sacrificial microcosms, (c) porosity as measured in test microcosms at the end of the experiment

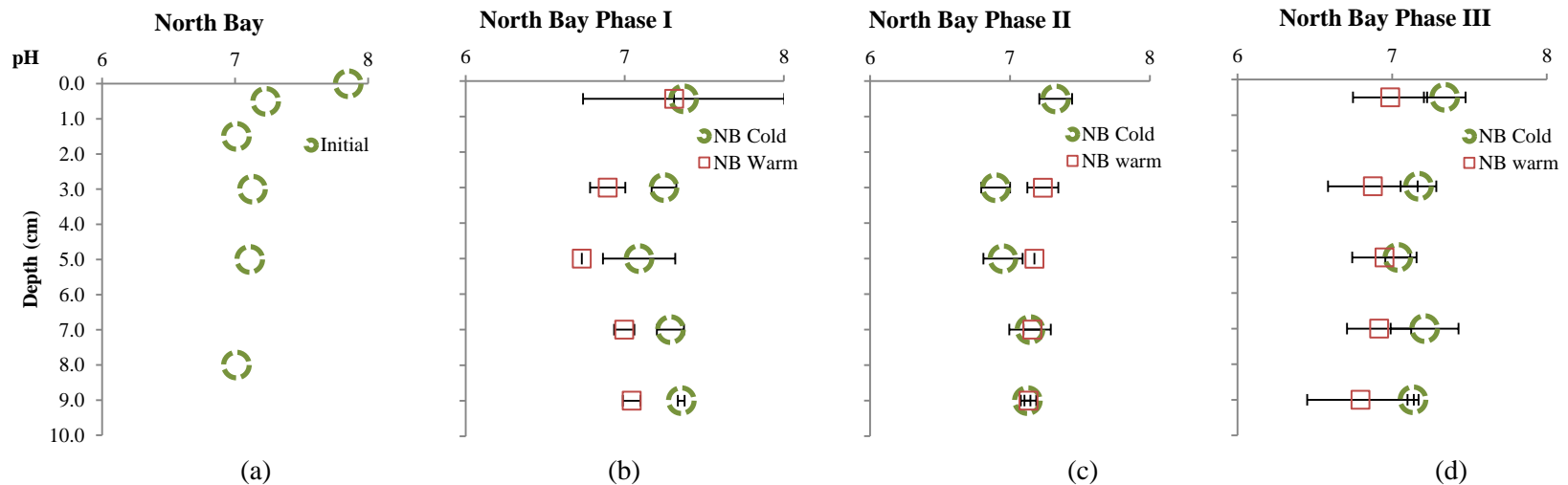


Figure 8 pH measurements taken from North Bay porewater samples taken at the end of each experimental Phase, (a) *in situ* conditions, (b) end of Phase I, (c) end of Phase II (d) end of Phase III

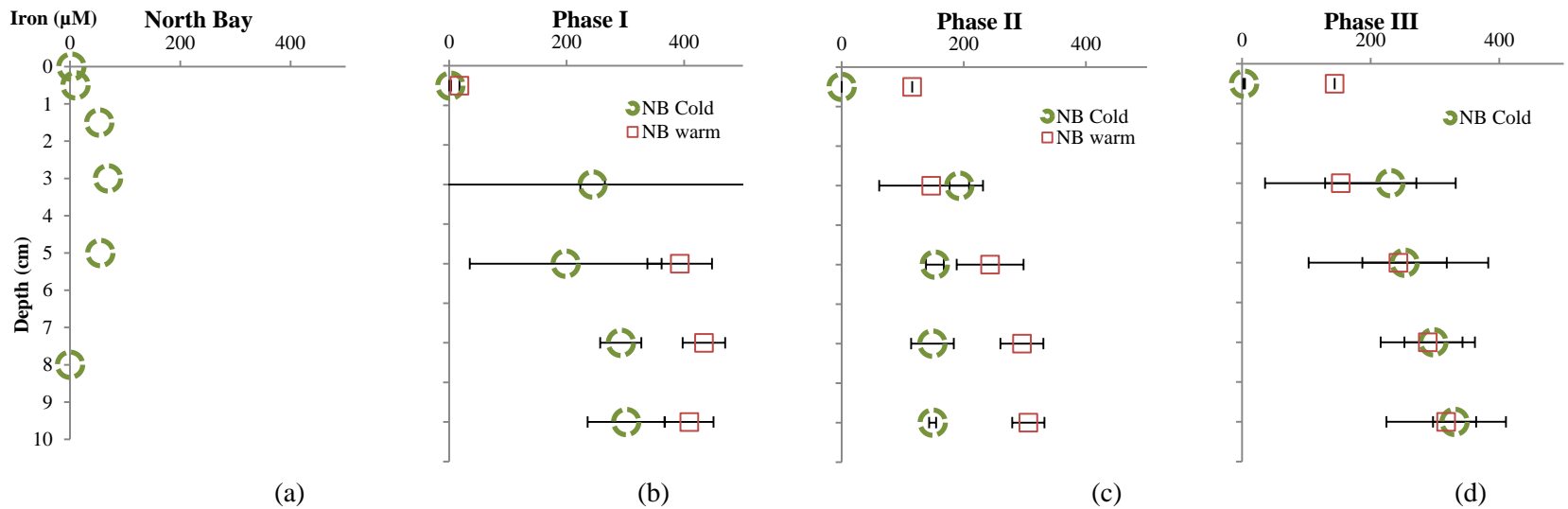


Figure 9 North Bay porewater iron measurements, units are in micromole/L, (a) *In situ* conditions, (b) end of Phase I, (c) end of Phase II, (d) and end of Phase III.

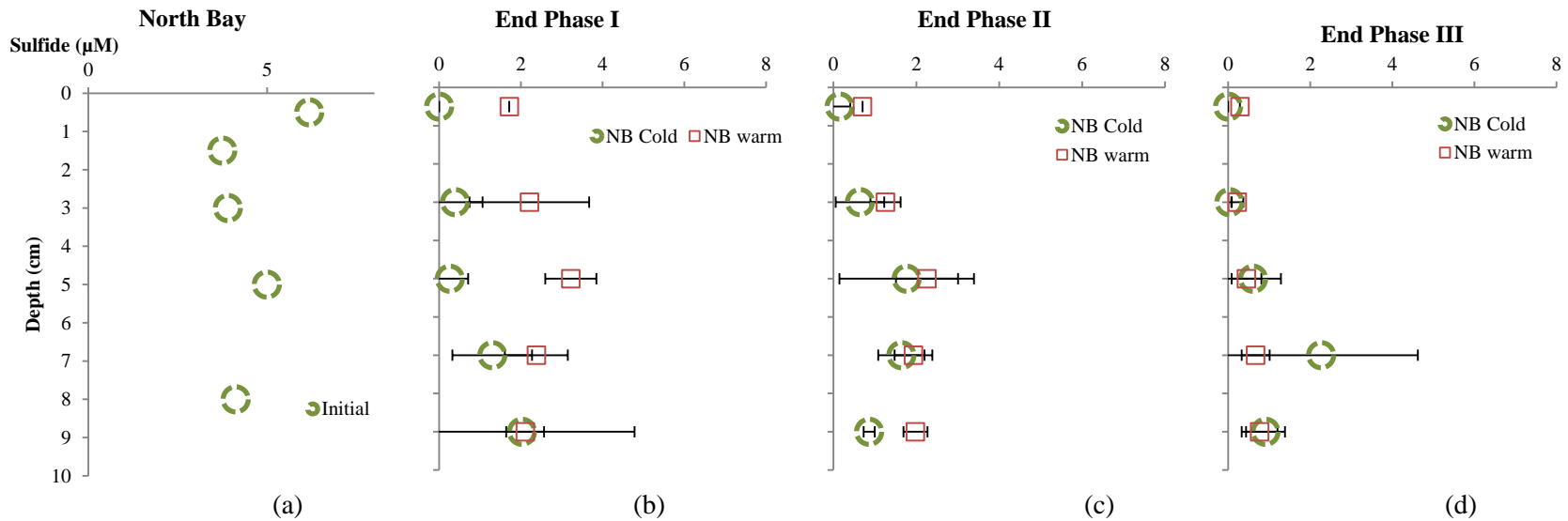


Figure 10 North Bay porewater sulfide measurements, units are in micromole/L, (a) *In situ* conditions, (b) end of Phase I, (c) end of Phase II, (d) end of Phase III

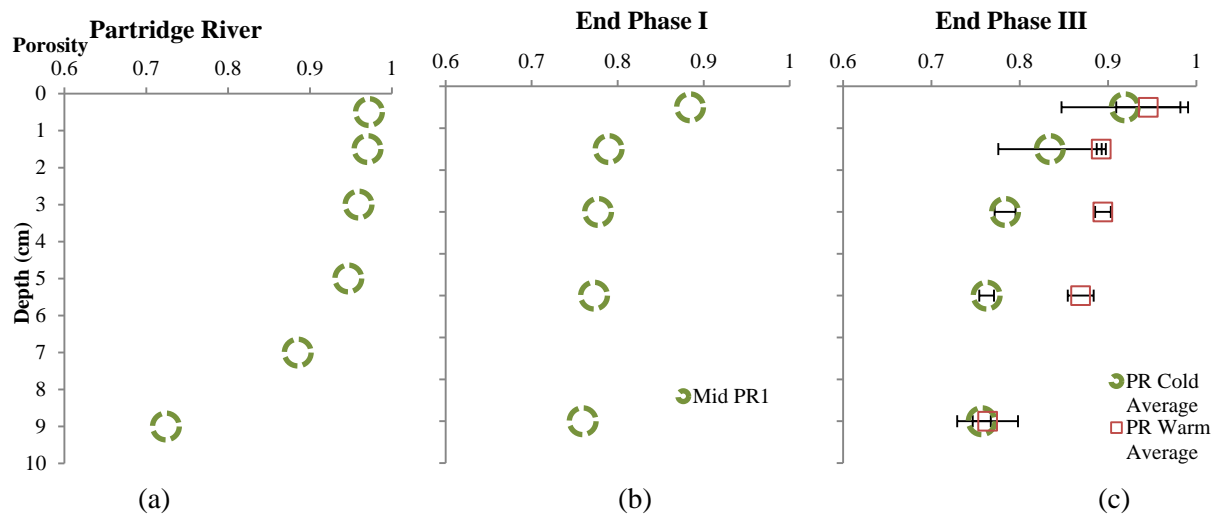


Figure 11 Porosity measurements based on moisture content depth profile of Partridge River sediments, (a) in- situ conditions, (b) mid way through experiment, sacrificial microcosms, (c) porosity as measured in test microcosms at the end of the experiment

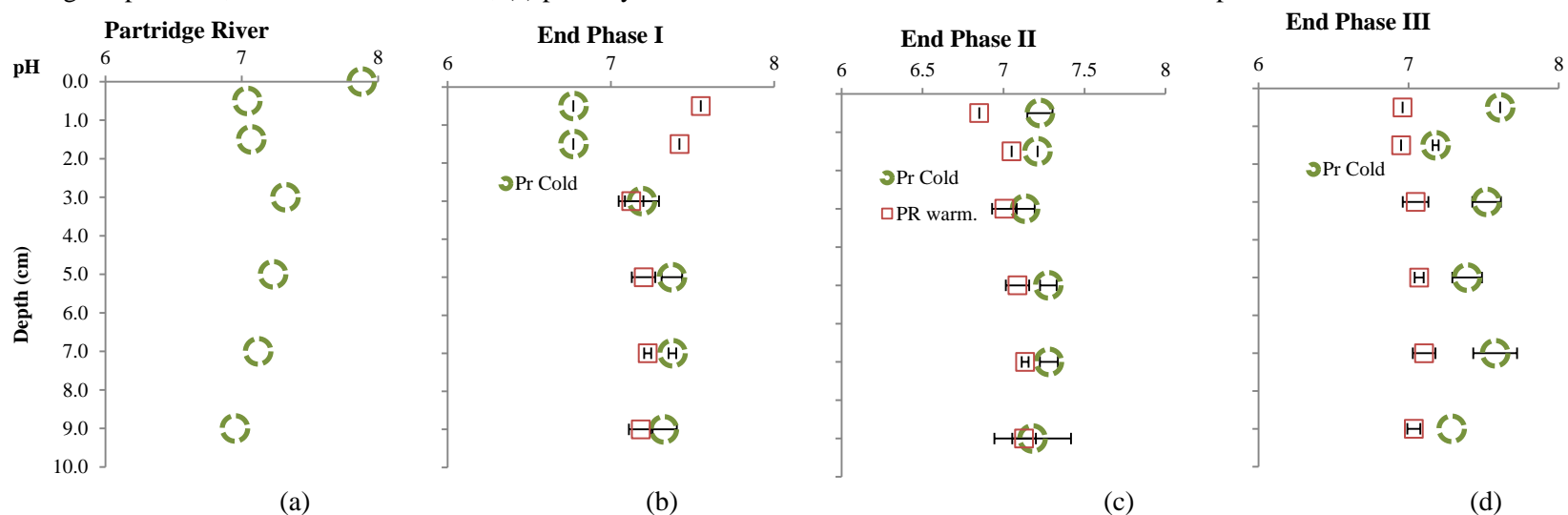


Figure 12 pH measurements taken from Partridge River porewater samples taken at the end of each experimental Phase, (a) *In situ* conditions, (b) end of Phase I, (c) end of Phase II, (d) end of Phase III

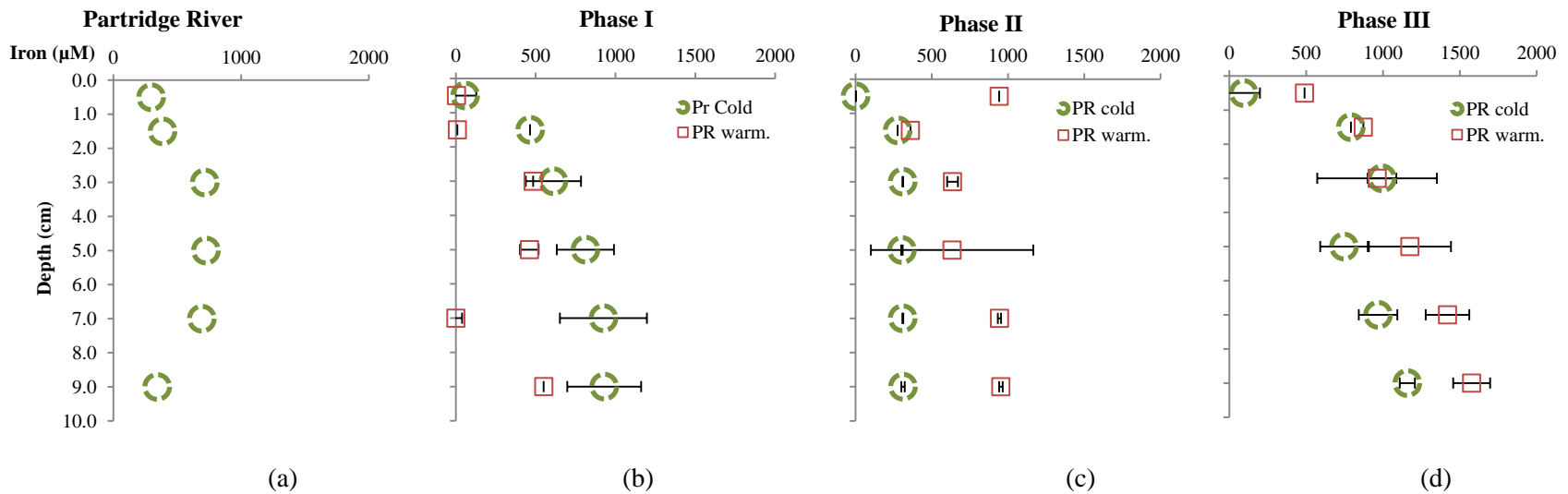


Figure 13 Partridge River porewater iron measurements, units are in micromole/L, (a) *In situ* conditions, (b) end of Phase I, (c) end of Phase II, (d) and end of Phase III.

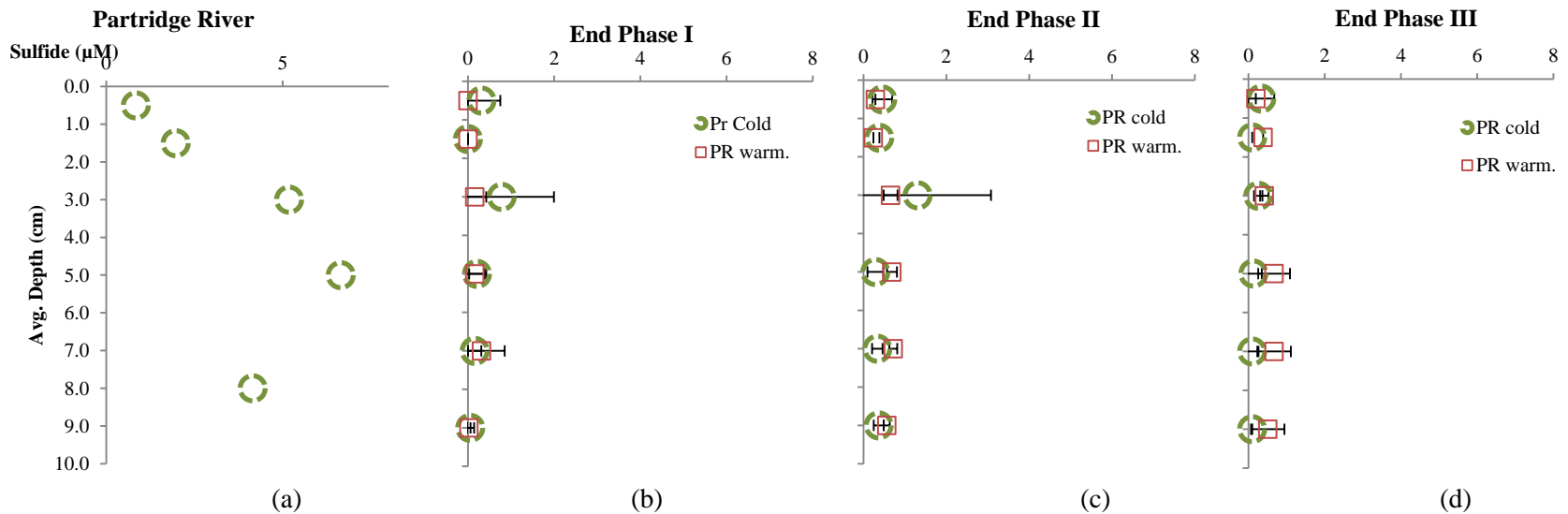


Figure 14 North Bay porewater sulfide measurements, units are in micromole/L, (a) *In situ* conditions, (b) end of experimental Phase I, (c) end of Phase II, (d) end of experimental Phase III

Sulfate Modeling Results

The first order reaction rate (0.15 / day) used for sulfate reactive transport modeling was constrained by the observation that porewater sulfate concentrations remained at roughly 30 % of overlying water concentrations at a depth of 3 cm in warm incubations at all times after 1 week during the loading phase. For cold microcosms, 30 % of the overlying water sulfate concentration was observed at roughly 3 cm after one week, but slightly deeper depths (4-5 cm) during weeks 6 and 9 (Figure 16a,b). After adjusting diffusion rates for temperature, a first order reaction rate of 0.040 /day for cold microcosms gave simulated porewater depth profiles of sulfate that matched experimental observations closely. The slowing of sulfate reduction with decreasing temperatures observed in this study ($Q_{10} = 2.0$ from calibration to observations) is on the low end of the range previously reported (Pallud and Van Capellen, 2006). Because observations were used to calibrate sulfate reduction rates, simulations of porewater sulfate concentrations during the loading phase (Fig. 16a,b) closely reflect observations in experiments (Figure 5, Appendix A, Figure 2).

Simulations calibrated to experimental observations produced estimates for instantaneous sulfate flux (at the sediment-water interface) and sulfate reaction (integrated over all depths) during loading and recovery phases (Figure 16c,d; Figure 17c,d). These instantaneous flux and reaction rates were summed to quantify the cumulative flux into sediment and the cumulative sulfate mass reduced in the sediments during the loading and recovery phases under both warm and cold conditions. Model simulation results for sulfate are presented only for North Bay since the lab experiments utilizing North Bay sediment more closely matched experimental objectives in which overlying water sulfate was constant during the loading phase (~300 mg/L) and remained low (<50 mg/L) for the recovery phase.

In the model simulation, there are three possible scenarios for sulfate molecules added to stationary sediment porewaters during a temporary loading phase: (1) they may accumulate in sediment pore fluids as sulfate, (2) they may react to form sulfide and remain in a dissolved or solid form, depending on iron concentrations in pore fluids, and (3) they may flux back out of sediment during the recovery phase (Figure 15, Appendix C). During the loading phase, net diffusional transport is positive in the direction of the sediment (negative dC/dx near the sediment-water interface) and this leads to an accumulation of sulfate in porewaters (Figure 16a,b). This accumulation of sulfate increases the rate of sulfate reduction in sediments since more is present to react in the porewaters. After some time during the loading phase, the diffusional transport into sediment matches the rate of sulfate reduction in the pore fluids. After this point in the loading phase simulation, accumulation in pore fluids ceases (Figure 16c,d) and any sulfate that diffuses into sediments reacts to form sulfide.

During the initial times of a recovery phase, the sulfate gradient is reversed (dC/dx is positive near the sediment-water interface), leading to a net diffusive transport out of the sediment and a loss of sulfate from pore fluids (Figure 15, Figure 17a,b). Sulfate continues to be reduced in the pore fluids during this phase, though reaction rates slow as less sulfate is present to react. After some time in the recovery phase, diffusion out of sediment and consumption of sulfate in porewater restores the negative sulfate gradient (Figure 17a,b), leading again to net diffusional transport into sediment (Figure 17c,d). Eventually net transport of sulfate into sediment matches reaction rates and this steady-state situation is then similar to that prior to the loading phase (Figure 16a,b).

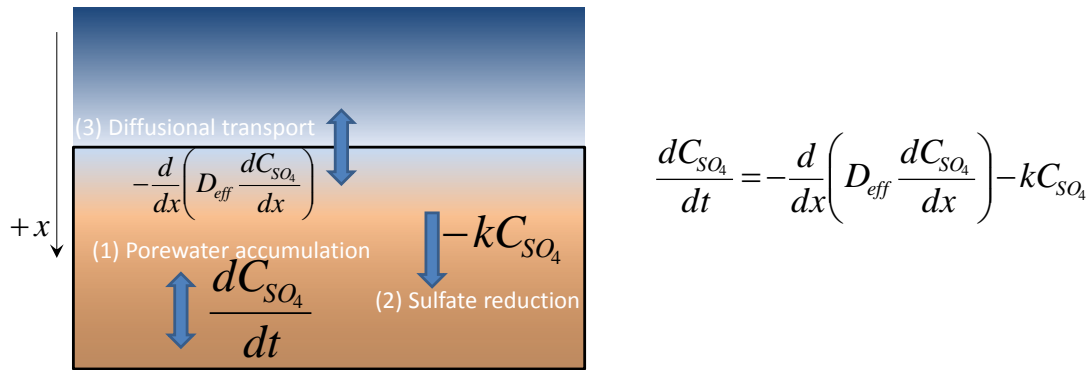


Figure 15 Mass balance and mathematical descriptions of processes transporting and transforming sulfate in sediments during loading and recovery phases.

Over the 80 day loading simulation (similar to the lab experiment's 11 week loading phase), model results showed an increase in sulfate in pore fluids from $48 \mu\text{g}/\text{cm}^2$ to $551 \mu\text{g}/\text{cm}^2$ for the warm system and from $88 \mu\text{g}/\text{cm}^2$ to $855 \mu\text{g}/\text{cm}^2$ for the cold system (Figure 16c,d, note log scale). During this same 80 day loading time, over $7,600 \mu\text{g}/\text{cm}^2$ sulfate was reduced to sulfide for the warm simulation, which amounted to over 94 % of the total sulfate flux into the sediment. Under cold conditions, $3,000 \mu\text{g}/\text{cm}^2$ were reduced over an 80 day loading period, representing 79 % of the total sulfate flux into the sediment (Figure 16c,d).

Over the first 4 weeks of the sulfate loading experiment, observations of sulfate concentrations in the overlying water of lab experiments suggested a total mass loss to sediments of $1.5 \text{ mg}/\text{cm}^2$ in North Bay cold microcosms and $2.3 \text{ mg}/\text{cm}^2$ for North Bay warm microcosms (Table 4). This is comparable to simulated cumulative sulfate mass fluxes of $1.6 \text{ mg}/\text{cm}^2$ for cold conditions after 28 days (58% of which was reduced), but less than the simulated cumulative mass flux of $3.1 \text{ mg}/\text{cm}^2$ over 28 days in warm conditions (84% of which was reduced). The assumption of a linear sulfate reaction rate ($0.15/\text{day}$) in the simple reactive transport model implemented here leads to an instantaneous sulfate loss rate of $38 \text{ mg L}^{-1} \text{ day}^{-1}$ for sulfate at $250 \text{ mg}/\text{L}$ for warm conditions, which is at the high end of the range of $4 - 40 \text{ mg L}^{-1} \text{ day}^{-1}$

day⁻¹ reported for maximum sulfate reduction rates in fresh and saltwater sediments (Pallud and VanCapellen, 2006). For cold conditions, the assumed linear reaction rate (0.040 / day) gives an instantaneous rate of 11 mg L⁻¹ day⁻¹ for sulfate at 250 mg/L, which is on the low end, but still within the reported range of maximum sulfate reduction rates.

Since appreciable increases in porewater sulfide were not observed in sediment pore fluids (Figures 10, 14), it is likely that any accumulation of sulfur in sediments occurred as solid-phase sulfides. Though the data to check this hypothesis are still being analyzed at the time of this report (AVS, total sulfur), a simple calculation can help determine what levels of sulfur accumulation would be expected. If it is assumed that the sulfur accumulation occurs uniformly in the upper 5 cm of sediment where sulfate reduction is most vigorous and that the bulk density of the sediment is roughly 0.5 g/cm³ (for an 80% porosity sediment having a particle density of 2.5 g/cm³), then this amounts to an accumulation of approximately 1,200 µg/g or 38 µmol/g total sulfur for cold simulations. These levels should be easily resolvable given the analytical limits of the techniques being utilized to quantify sulfur in the solid phase.

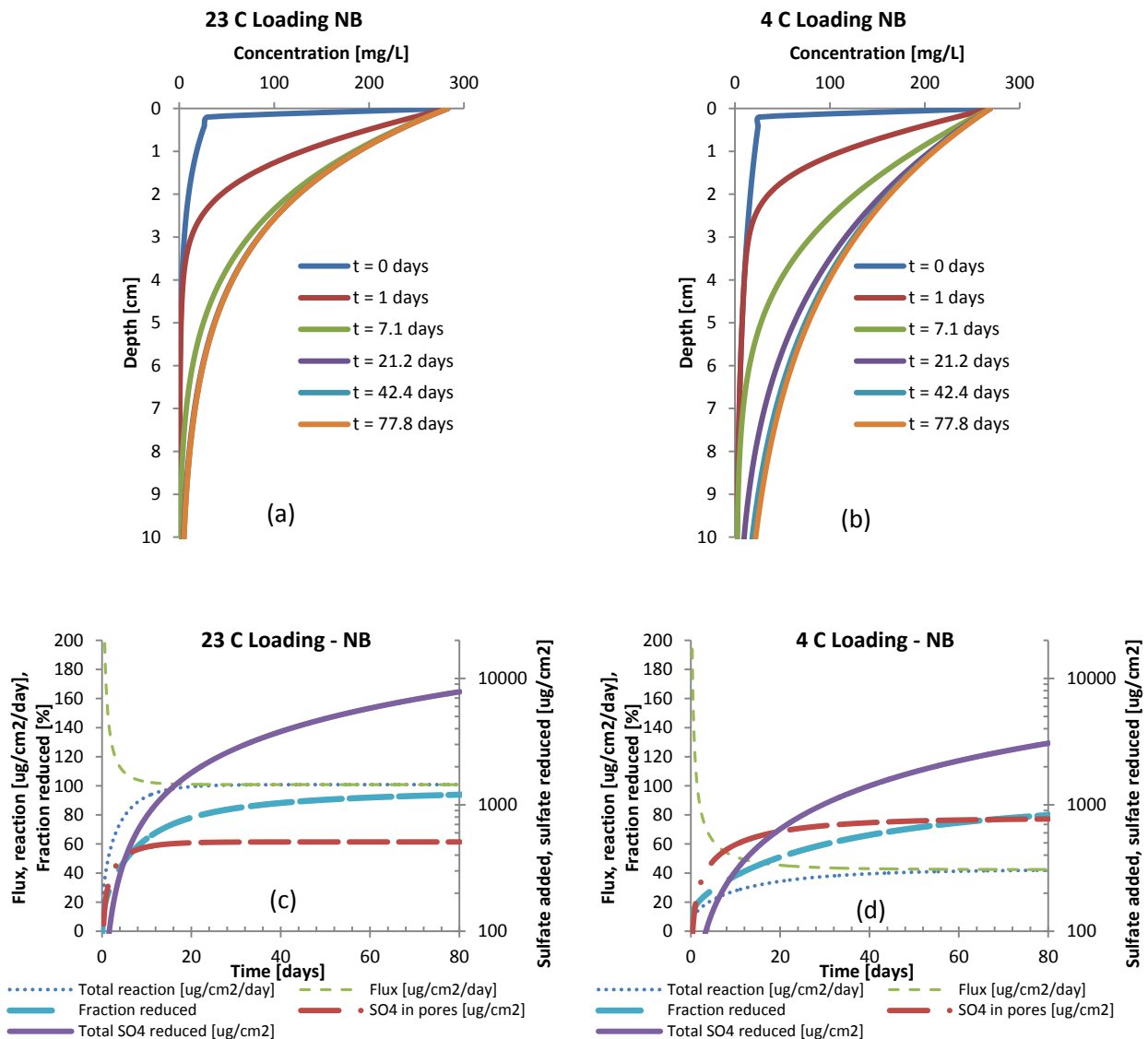


Figure 16 Model simulated porewater concentrations in (a) warm and (b) cold microcosms during sulfate loading phase of lab experiments. Model simulated flux across the sediment-water interface and reaction in (c) warm and (d) cold microcosms during sulfate loading phase of lab experiments.

Similar to observations made during the experimental recovery Phase III (Figure 5, Appendix A Figure 2), simulated gradients in porewater sulfate concentration were reversed following a decrease in overlying water sulfate. Sulfate near the sediment water interface diffused out of the sediment while reactions within the sediment were still consuming sulfate (Figure 17a,b). These combined sulfate loss mechanisms are both affected by temperature and led to different lengths of time before the downward diffusional gradient of sulfate was restored in the simulated warm (2.6 days, Figure 17a, c) and cold (12.5 days, Figure 17b,d) conditions.

Since overlying water sulfate concentrations remained elevated during the recovery phase, particularly for the warm Partridge River microcosms, porewater sulfate observations in Figure 5 are normalized to the average overlying water sulfate concentration for the preceding week. These observations clearly show that porewater sulfate concentrations in excess of those in the overlying water persisted in cold microcosms for longer than in the warm microcosms due to relatively slower diffusion and reaction rates. While observations showed porewater sulfate concentrations in excess of surface water sulfate persisted in cold microcosms for over 4 weeks during Phase III (Figure 5e,j), simulations showed porewater sulfate similar to overlying water sulfate at all depths in cold conditions after only 2 weeks (Figure 17b). The observation of elevated sulfate in microcosm porewater after 4 weeks in cold conditions suggests that temperature may have affected sulfate reduction rate more than model simulations predict.

Depending on temperature, simulations showed that a total of 3,800 (cold) and 7,800 (warm) $\mu\text{g}/\text{cm}^2$ sulfate was added to sediment (fluxed across the sediment-water interface) during the loading phase (Figure 16c,d). These numbers are consistent with independent, empirical estimates made from overlying water observations over the first 4 weeks (Table 4). In warm conditions, model results showed that of the 7,800 $\mu\text{g}/\text{cm}^2$ total sulfate that fluxed into the sediment during the 80 day loading phase, only 305 $\mu\text{g}/\text{cm}^2$ sulfate accumulated in sediment pore fluids (Figure 16c). The remainder reacted to form sulfide, which was likely immediately converted to solid phase iron sulfide due to the high iron concentrations in sediment pore fluids. Over 2.6 days of recovery in warm conditions, 198 $\mu\text{g}/\text{cm}^2$ of the 305 $\mu\text{g}/\text{cm}^2$ sulfate added to pore fluids during the loading phase was removed via reaction (82 $\mu\text{g}/\text{cm}^2$) and flux out (116 $\mu\text{g}/\text{cm}^2$) (Figure 17c). In cold conditions, model results showed that of the 3,800 $\mu\text{g}/\text{cm}^2$ of total sulfate that fluxed into the sediment during the 80 day loading phase, only 742 $\mu\text{g}/\text{cm}^2$ sulfate accumulated in sediment pore fluids (Figure 16d). The remainder reacted to form sulfide, which was immediately converted to solid phase iron sulfide. Over 12.5 recovery days in the cold conditions, 486 $\mu\text{g}/\text{cm}^2$ of the 742 $\mu\text{g}/\text{cm}^2$ sulfate added to pore fluids during the loading phase was removed via reaction (247 $\mu\text{g}/\text{cm}^2$) and flux out (239 $\mu\text{g}/\text{cm}^2$) (Figure 17d). Specific accounting of sulfate after the downward diffusional gradient in sulfate is restored (predicted to be 2.6 days in warm conditions, 12.5 days for cold) becomes complicated since some sulfate in pore fluids remains there as a result of the loading phase, but other sulfate is present due to diffusion in during the recovery phase. However, once the downward diffusional gradient is restored, no sulfur added to sediment during the loading phase will be released back to surface waters via passive molecular diffusion. This puts an upper bound on the amount of sulfate which was added to pore fluids during the loading phase that could be released back to the overlying water.

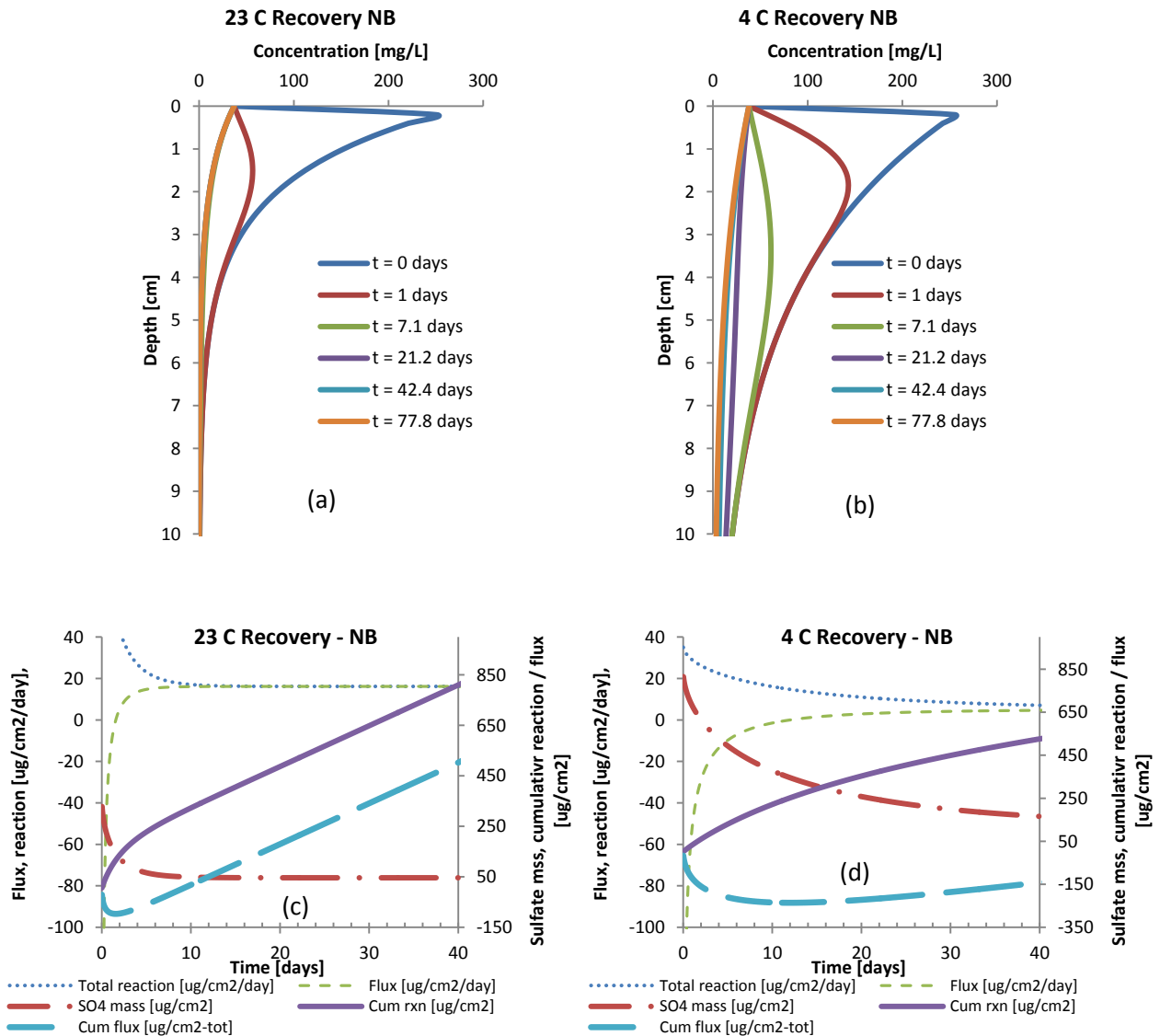


Figure 17 Model simulated porewater concentrations in (c) warm and (d) cold microcosms during sulfate recovery phase of lab experiments. Model simulated flux across the sediment-water interface and reaction in (a) warm and (b) cold microcosms during sulfate recovery phase of lab experiments.

In both loading and recovery phases, sulfate flux into sediment eventually matched reaction in sediment, leading to a steady state amount of sulfate in pore fluids. However, the reaction of sulfate to sulfide continued to cause an accumulation of sulfur in the sediment, presumably in the form of iron-sulfide minerals. Simulated rates of steady accumulation of sulfur in the sediment (solid phases) under warm and cold loading and recovery scenarios show rates 7-10x faster during a 300 mg/L loading phase than during a ~40 mg/L recovery phase (Table 7). Simulated warm conditions (23 °C) have accumulation rates of sulfide in sediment (solid phases) 2.5 – 3.5 times faster than cold (4 °C) conditions.

Table 7 Simulated steady state sulfate flux under cold and warm loading and recovery conditions

	Cold steady state flux	Warm steady state flux
	[ug cm⁻² day⁻¹]	[ug cm⁻² day⁻¹]
Loading Phase (~300 mg/L overlying water)	42.5	100.8
Recovery Phase (~40 mg/L overlying water)	4.6	16.2

Since simulations carried out for sulfate flux and reaction relied on model coefficients calibrated to lab settings, it is unrealistic to assume that the modeled results can be confidently extrapolated to field conditions. However, model results are instructive in that they reveal that, regardless of adjustments of diffusion and reaction rates to field conditions, a great majority of the sulfate that diffuses into sediments during an ~80 day loading phase is likely to be reduced to sulfide in either warm or cold conditions. The quantity of sulfate that diffuses out of sediment will represent a larger fraction of the total sulfate added to the sediment if a recovery phase occurs during cold conditions; however, the sulfate that diffuses out of sediment during a recovery phase is not likely to represent a majority of the sulfate that diffused in during the loading phase unless the loading phase is very short. As an example, after 8 days of simulated cold loading, 450 ug/cm² had accumulated in pore fluids while only 130 ug/cm² had reacted. After 30 days, however, 680 ug/cm² had accumulated in pore fluids while 1000 ug/cm² had reacted.

The reactive transport model used in this report does not directly account for the accumulation of sulfide in sediments, but assumes that any sulfate that was reduced in sediment is reduced to sulfide (rather than an intermediate sulfur phase) and is immediately trapped in sediments as a solid-phase sulfide. This assumption is reasonable for completely stationary sediment containing sufficient iron to maintain oversaturation with respect to iron-sulfide minerals. However, this assumption was clearly violated in the case of the warm Partridge River sediment microcosms in which oxidation of iron sulfide minerals as a result of bioturbation likely re-mobilized solid phase sulfides. A riverine system is likely to have a sediment bed which is not completely stationary, and interpretation of the experimental and mathematical results presented here in the context of natural systems should consider more fully the biological and hydrological processes which could result in re-mobilization of sulfide minerals associated with the solid phase.

Sulfate diffusing out of sediment pore fluids during a recovery phase has the potential to influence a stream's water column sulfate concentration. An example calculation was made based on a 6.2 km stretch of a 30 m wide stream carrying 0.3 cubic meters per second of low sulfate (< 20 mg/L) water. If 250 ug/cm² was released from sediments during the first 7 days of a recovery phase (Figure

17c), sulfate concentration in stream water would increase by 2.6 mg/L over a distance of 6.2 km. This increase in river sulfate is proportional to the mass of sulfate released from sediment pore fluids per unit area, the width of the river, and the length of the river. It is inversely proportional to the flow of the river and the time required for sulfate to flux out. If sediment porewater reaches steady state with respect to sulfate during the loading phase (simulations suggest ~20 days for warm conditions and ~60 days for cold conditions), the mass of sulfate in the sediment is proportional to the overlying water sulfate concentration during the loading phase and inversely proportional to the square root of the ratio of k (first order sulfate reaction rate) and D (effective sediment diffusion). Assuming half of the sulfate mass per unit area in pore fluids diffuses out prior to reacting in sediments, the concentration increase in a stream during the beginning of a recovery phase can be estimated as:

$$\Delta C = \frac{0.5 \left(\frac{C_{load}}{\sqrt{\frac{k}{D}}} \right) WL}{Qt}$$

Where

- C_{load} is the concentration of overlying water sulfate during the loading phase (assume porewater reaches steady state) [$\mu\text{g}/\text{cm}^3$] or [mg/L]
- k is the first order sulfate reaction rate [/day]
- D is the effective sulfate diffusion in sediment [cm^2/day]
- W is the stream width [cm]
- L is the stream length [cm]
- Q is the flow of the river [L/day]
- t is the time necessary for sulfate to diffuse out of sediment [day]
- ΔC is the change in stream concentration [$\mu\text{g}/\text{L}$]

This change in concentration could be important for very slow moving or particularly long streams. However, a recovery phase timed to be coincident with high flows during spring snow melt would make large increases in stream sulfate concentrations due to release from sediment pore fluids unlikely in most cases.

4. Conclusions

Sulfur is a naturally occurring element that, in particular forms, has the potential to be detrimental to the production of wild rice. This study provides a temperature dependent model for rates of sulfate transport and reaction in sediments in response to seasonal sulfate loading in the overlying water. The laboratory set up for this experiment provided a controlled environment for studying the influence of temperature on sulfate diffusion into and out of sediment porewaters. Variables such as sediment disturbance, oxygen production via photosynthesis, and advective fluid movement were largely eliminated in an attempt to simulate a simplified natural system.

Overall, effective diffusion for tracers in lab experiments proceeded at a rate similar to modeled results, and occurred only slightly more rapidly under warm conditions than under cold conditions, regardless of sediment type (Figures 3, 4, and, 6, Appendix B, Table 1). Even though the diffusion of the tracers occurred more rapidly into the warm sediments than the cold sediments, normalized sulfate concentrations (Figure 5) were slightly higher at all depths within the cold sediments when compared to the warm sediments. These higher cold porewater concentrations are indicative of higher rates of sulfate reaction within the warm sediments. With regard to the early part of the recovery phase, porewater sulfate concentrations in cold microcosms were typically three times higher than warm porewater concentrations at comparable depths (Figure 5). The experiment was set up to monitor the transfer of sulfate from the surface waters into the porewaters, resembling a natural system. This experiment did not take into consideration groundwater flow or temperature fluctuations a natural system would see. Since the sediment used for the experiment did come from natural systems, some of the mud-dwelling organisms were noticed burrowing within the microcosm throughout the experiment, similar to a natural system.

Phase II provided a means of quantifying dissolved sulfate within the porewaters at a given time based on the surface water concentration. This is of interest due to the predilection of bacteria to reduce sulfate to sulfide under anoxic conditions (Van Der Well, Smolders, OP Den Camp, Roelofs & Lamers, 2007). Though porewater sulfide was measured initially and at the end of each phase, a quantifiable rise in dissolved sulfide was not observed over the course of this nine-month study. A similar study conducted by Van der Well et al. 2007, observed a strong negative relationship between iron and sulfide concentrations within sediment porewaters. Their research was conducted over the course of 21 months and utilized *in situ* testing within a peat meadow.

Based on the geochemistry of the sediments used for the present study where iron concentrations of 200 – 1000 uM were observed, low sulfide concentrations could be expected (Van Der Well et al. 2007), based on the formation of insoluble iron sulfide compounds. The initial hypothesis for the present

study was that a decrease in porewater iron would be observed during the loading phase of the study as iron sulfide was formed; however, the sulfate exposure portion of this study was not long enough to allow a measurable titration of the high iron content (including solid phase) of the sediment and the appreciable accumulation sulfide in the porewaters. A longer-term sulfate loading study was conducted in field mesocosms as a part of the MPCA Wild Rice Sulfate Standard Study and is described in separate reports (Johnson 2014; Pastor and Dewey 2013). Though the field mesocosm studies contained a longer time course of sulfate loading, they occurred in hydrologically isolated tanks and therefore cannot capture the effects of groundwater or other sulfur and iron sources to natural field sites.

The observation and modeling results presented here show that over an 80 day sulfate loading phase, a vast majority of the sulfate added to sediment reacts to form sulfide, even at 4 °C when biological rates are slower. The observations and modeling suggest that the primary benefit of extended (greater than about 4 weeks) sulfate releases to surface waters during cold conditions, from the standpoint of minimizing sulfur accumulation in sediments, is due to slower reaction rates rather than outward diffusion of sulfate during a recovery phase. Detailed calculations were not made for different scenarios, but the modeling results suggest that if the loading phase was shorter, a smaller fraction of the sulfate mass transported into sediments would be reacted and a larger fraction would be transported out during a recovery phase. Higher surface water concentrations during the loading phase would be required to release an equivalent mass of sulfate in a shorter time, and more detailed simulations would be required to evaluate the implications of overlying water concentration and loading phase duration.

While the sulfate molecule itself is relatively unreactive under oxidizing conditions, sufficient quantities of sulfate in the overlying water can lead to appreciable diffusional transport into freshwater aquatic sediment. The reactivity of sulfide – a byproduct of biological sulfate reduction – in anoxic conditions can fundamentally change the geochemical and biological processes that occur in freshwater sediments containing sufficient labile organic matter to support bacterial activity. Elevated sulfate levels in the porewaters provide favorable conditions for sulfate reducing bacteria that, over time, could produce sulfide in excess of the iron availability in a system and result in an accumulation of dissolved sulfide in pore fluids (Johnson 2014). Sufficient quantities of dissolved sulfide could have detrimental effects on aquatic vegetation and organisms. This study provided both a physical and mathematical model to describe the porewater sulfate response to seasonal sulfate loading into surface water under different temperatures. These results will help to answer the question of how much sulfate diffuses into, and reacts within sediment, as a function of temperature and inform management decisions regarding the timing of sulfate release to natural waterways.

5. Acknowledgements

Dr. Nathan Johnson, University of Minnesota Duluth, Dr. Edward Swain and Phil Monson, of the Minnesota Pollution Control Agency, were instrumental throughout the entire experiment, providing key insight into the experimental design as well as the presentation of results, and being a helping hands through the countless, and sometimes cold, hours of sampling, data processing and report editing. Dr. Sergei Katsev of the University of Minnesota has provided insight and experience to the authors throughout the modeling portion of this experiment. Ryan Armstrong, undergraduate of the University of Minnesota Duluth, Brian Beck and, Sean Rogers of LacCore UMN, have provided much appreciated assistance throughout the sample collection and have aided in the smooth progression of this experiment.

6. References

- Boudreau, B. P. (2003). *Diagenetic models and their implementation, modelling transport and reactions in aquatic sediments*. (1st ed.). New York, NY: Springer.
- Eaton, A. Clesceri, L., Rice E., and Greenberg, A., (Eds.), (2005)a. 3500-Fe-B Phenanthroline Method. In *Standard Methods for the examination of water and wastewater* (21 ed.). Baltimore, Maryland: Port
- Eaton, A. Clesceri, L., Rice E., and Greenberg, A., (Eds.), (2005)b. 4500-S²⁻ D. Methylene Blue Method. In *Standard Methods for the examination of water and wastewater* (21 ed.). Baltimore, Maryland: Port
- Eaton, A. Clesceri, L., Rice E., and Greenberg, A., (Eds.), (2005)c. 4110 C. Single Column Ion Chromatography. In *Standard Methods for the examination of water and wastewater* (21 ed.). Baltimore, Maryland: Port
- Fairbrother, A., & Wentzel, R. Environmental Protection Agency, (2007). *Framework for metals risk assessment* (EPA 120/R-07/001). Retrieved from Office of the Science Advisor website: <http://www.epa.gov/raf/metalsframework/pdfs/metals-risk-assessment-final.pdf>
- H. Fossing, T.G. Ferdelman, P. Berg, (2000) Sulfate reduction and methane oxidation in continental margin sediments influenced by irrigation (South-East Atlantic off Namibia), *Geochim. Cosmochim. Acta* 64 (5) 897–910.
- Johnson, N. W. (2013) Response of rooting zone geochemistry to experimental manipulation of sulfate levels in Wild Rice mesocosms. MPCA Report. December 2013.
- Minnesota Pollution Control Agency, (2013)a. *Minnesota's sulfate standard to protect wild rice*. Retrieved from website: <http://www.pca.state.mn.us/index.php/water/water-permits-and-rules/water-rulemaking/minnesotas-sulfate-standard-to-protect-wild-rice.html>
- MPCA, (2013)b, *Wild Rice Sulfate Standard Sediment Incubation Experiment – Quality Assurance Project Plan*. Retrieved from website: <http://www.pca.state.mn.us/index.php/view-document.html?gid=20337>
- Minnesota Pollution Control Agency, Environmental Outcomes Division. (1999). *Sulfate in Minnesota's ground water*. Retrieved from website: <http://www.pca.state.mn.us/index.php/view-document.html?gid=6308>
- Minnesota Pollution Control Agency, (2011). *The sulfate standard to protect wild rice study protocol* (wq-s6-42b). Retrieved from website: <http://www.pca.state.mn.us/index.php/view-document.html?gid=16356>
- Pallud, C., and Cappellen, P. V. (2006). Kinetics of microbial sulfate reduction in estuarine sediments. *Geochimica et Cosmochimica Acta* 70:1148-1162.

Pastor, J., and Dewey, B. (2013) Effects of enhanced sulfate concentrations on wild rice populations. MPCA Report, December 2013.

Seeberg-Elverfeld, J., Schluter, M., Feseker, T., & Kolling, M. (2005). Rhizon sampling of porewaters near the sediment-water interface of aquatic systems. *Limnology and oceanography: Methods*, 3, 361-371.

Van Der Well, M. E. W., Smolders, A. J. P., OP Den Camp, H. J. M., Roelofs, J. G. M., & Lamers, L. P.

M. (2007). Biogeochemical interactions between iron and sulphate in freshwater wetlands and their implications for interspecific competition between aquatic macrophytes. *Freshwater Biology*, 52(3), 434-447.

7. Appendix A.

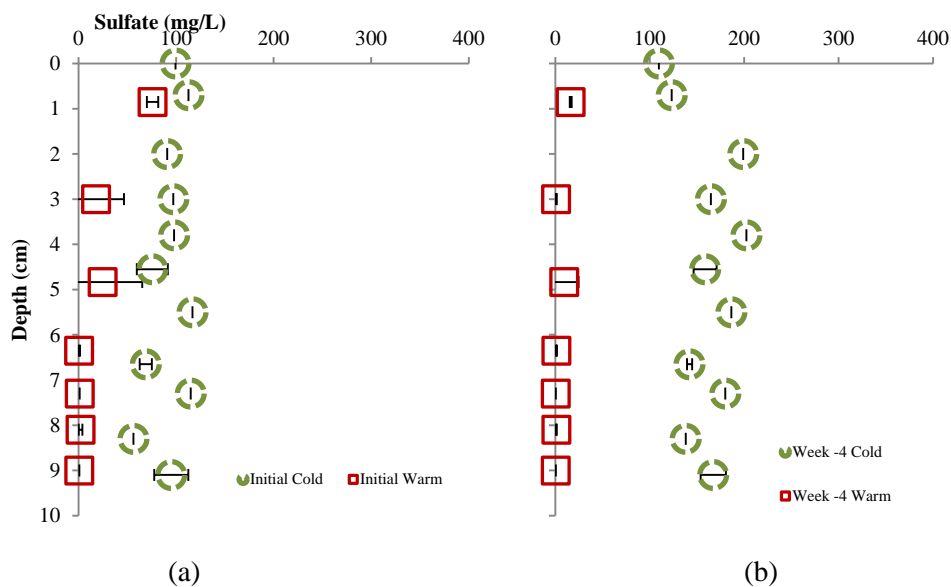
Table 1. Outline of experimental schedule with dates of important experimental considerations, anion amendment, surface water replacement and porewater sampling

Phase	Week (dates)	Anion Spike	Water Replacement	Surface water samples	Porewater sampling
Equilibrium	0 (2/20)			2/20	
	1 (2/25)			2/27	
	2 (3/4)		3/8PR	3/5	
	3 (3/11)			3/11	
I Chloride (Cl⁻)	0 (3/11)	3/13			3/12,3/15
	1 (3/17)	3/20	3/20PR	3/19	
	2 (3/25)			3/26	
	3 (4/1)			4/2	4/9-4/10
	4 (4/8)			4/8	
	5 (4/15)		4/15	4/15	
	6 (4/22)			4/22	
II Fluoride (F⁻) Sulfate (SO₄⁻)	0 (4/22)	4/23		4/24	4/30
	1 (4/29)		4/29 PR	4/30	
	2 (5/6)			5/7	
	3 (5/13)	5/17		5/13	
	4 (5/20)	5/23		5/20	
	5 (5/27)			5/28	6/4
	6 (6/3)			6/3	
	7 (6/10)			6/10	
	8 (6/17)			6/17	6/25
	9 (6/24)	6/28*	6/28	6/26,6/28	
	10 (7/1)				
11 (7/8)		7/9	7/8,7/9,7/12		
III Bromide (Br⁻)	0 (7/15)			7/15,7/17	7/16
	1 (7/22)			7/24,7/24,7/28	
	2 (7/29)	7/15,7/17	7/17		
	3 (8/5)	7/24	7/24		8/5
	4 (8/12)	7/29	7/29	8/5	
	5 (8/19)			8/12	
	6 (8/26)			8/20	
	7 (9/2)	8/21	8/21 PR	8/29	9/5
	8 (9/9)			9/6	
			9/9		

Table 2 Overlying water sulfate concentrations [mg/L] used to normalize porewater sulfate in Figure 5.

	PR Cold	PR Warm	NB Cold	NB Warm
Week 1	103.7	80.9	30	37.3
Week 6	284.3	296.4	281.4	261.8
Week 9	292.6	411.3	288.6	323.9
Week 9	223.8	450.1	245.0	273.4
Week 12	82.4	241.7	139.9	133.9
Week 15	22.3	87.2	15.6	22.3
Week 19	35	102.3	23.9	25.2

Phase I PR



Phase 1 NB

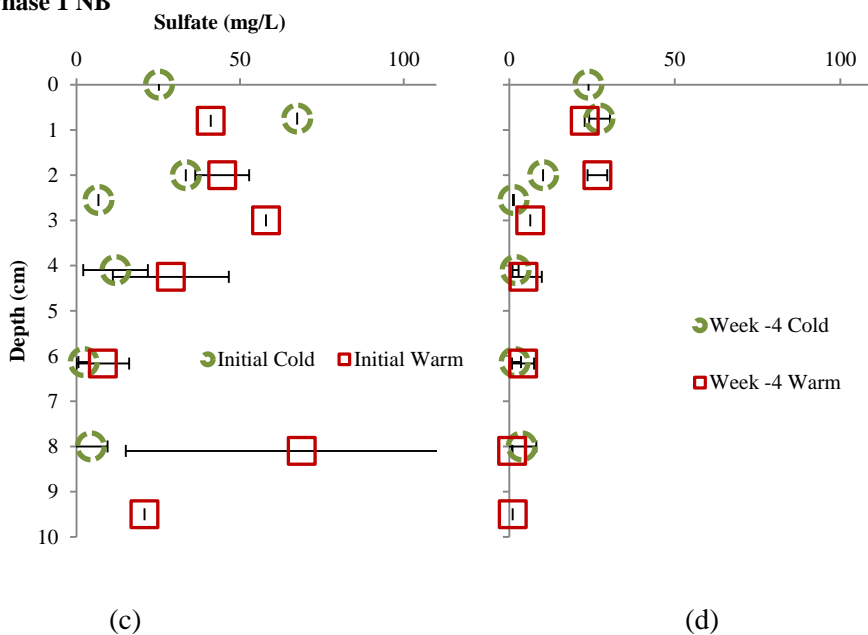


Figure 1 Sulfate concentrations during Phase I. Note that the subplots show the transition between Phase I and II and the times specified are relative to the initiation of Phase I. (a) Partridge River initial conditions at the beginning of Phase I (b) Partridge River porewater four weeks after the start of Phase I (c) North Bay initial conditions at the beginning of Phase I (d) North Bay four weeks after the start of Phase I

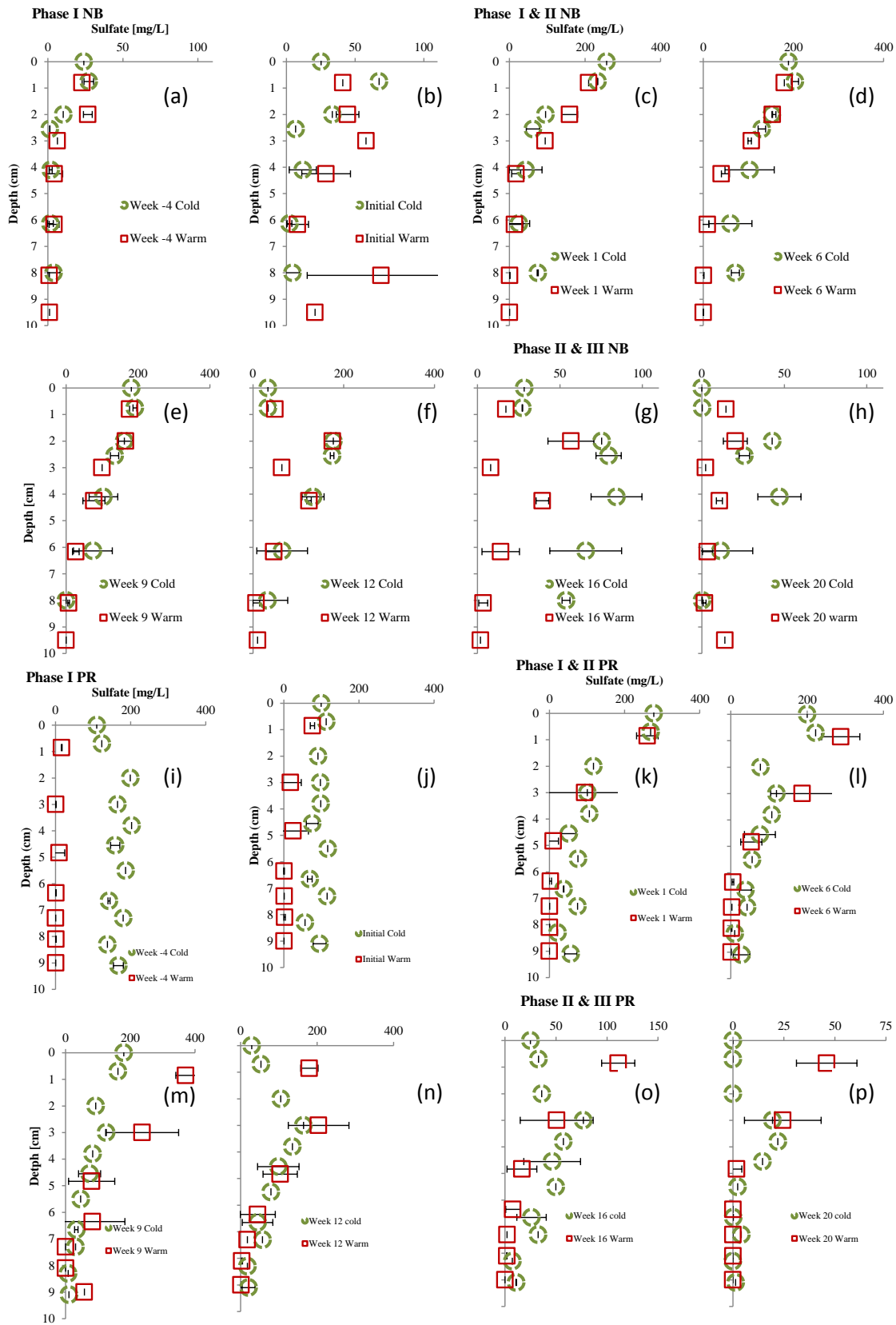


Figure 2 Raw (not normalized) porewater sulfate concentrations during all phases in (a-h) North Bay and (i-p) Partridge River microcosms.

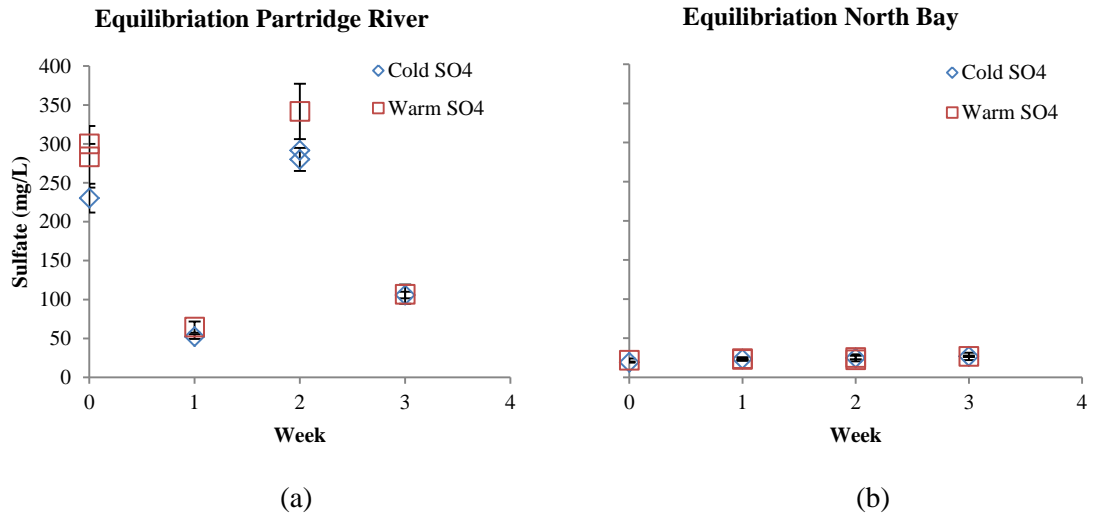


Figure 3 Sulfate levels in overlying water during the equilibration period (a) Partridge River (b) North Bay

8. Appendix B

Mathematical procedure to develop the model for chloride, fluoride and bromide tracers

The Boudreau diffusional coefficients depend on sediment porosity, with equations outlined below

$$\text{Porosity}^* (\varphi) = (\text{volume of water})/(\text{total sediment and water volume}).$$

$$D^o = (m_o + m_1 * T) * 10^{-6} \text{ cm}^2/\text{s}$$

$$D' = \frac{D^o}{\theta^2}$$

$$\theta^2 = 1 - b * \ln(\varphi)$$

D^o is the temperature dependent anion diffusion coefficient (cm^2/sec)

T is the environmental temperature ($^{\circ}\text{C}$)

D' is the effective diffusion rate (cm^2/sec)

θ^2 is the sediment tortuosity

γ is sediment porosity

b is a constant (≈ 2.02)

$$\text{Porosity}^* (\varphi) = \frac{W_w}{\gamma_w} / \left(\frac{W_s}{\gamma_s} + \frac{W_w}{\gamma_w} \right)$$

γ_s =unit weight of soils ($18\text{kN}/\text{m}^3$ for North Bay sediment, $16\text{kN}/\text{m}^3$ for Partridge River)

γ_w is the unit weight of water

W_s is the weight of solids

W_w is the weight of water

* porosity calculation assumes fully saturated conditions.

Table 1 Diffusional coefficients, cm^2/sec . (Boudreau, 2003)

	Cold (From Calibration)	Warm (From Calibration)	Cold (Theoretical)	Warm (Theoretical)
Bromide	1.50E-05	2.12E-05	1.20E-05	1.88E-05
Chloride	1.16E-05	1.184E-05	1.16E-05	1.84E-05
Fluoride	1.86E-06 ^a	3.39E-06 ^a	7.83E-06	1.32E-05
Sulfate	7.50E-06 ^b	1.06E-05 ^b	5.92E-06	9.52E-06

^a Fluoride effective diffusion from calibration to porewater observations likely influenced by low overlying water concentrations early during Phase II

^b Effective sulfate diffusion coefficients extrapolated from effective bromide (non-reactive) diffusion quantified during Phase II using temperature and molecular-weight dependence

Transport model:

Starting with the standard second order advection-diffusion-reaction partial differential equation describing a change in concentration in a one-dimensional spatial domain as a function of time,

$$\frac{dC}{dt} = -u * \frac{dC}{dx} + D * \frac{d^2C}{d^2x} - kC$$

and discounting the advective flow and reaction term (u-advective flow and -kC, reaction)

$$\frac{dC}{dt} = D * \frac{d^2C}{d^2x}$$

Then by estimating numerical values for the change in concentration of a particular distance using central differences,

$$\frac{dC}{dx} = \frac{C_{i+1} - C_{i-1}}{(2 * \Delta x)}$$

$$\frac{d^2C}{d^2x} = \frac{C_{i+1} - 2 * C_i + C_{i-1}}{(\Delta^2 x)}$$

ending with

$$\frac{dC}{dt} = D * \frac{C_{i+1} - 2 * C_i + C_{i-1}}{(\Delta^2 x)}$$

where dC is the change in concentration

u is the advective fluid movement

dx is the distance between two points of interest

D is the diffusional coefficient

kC is the reaction term for the species of interest

dt is the change in time

Boundary and initial conditions for tracer simulations are as follows:

BC: $C(x=0,t) = C_{\text{surface water}}$

BC: $dC/dx|_{(x=L,t)} = 0$

$C(x,t=0) = 0$

9. Appendix C.

Reactive transport model formulation for sulfate

Simple numerical solution for transient advection, diffusion, first order reaction equation with coefficients potentially varying in space. When applied to laboratory microcosms, advective velocity was set to zero. The initial condition – $f(x)$ for Phase II was set to numerical estimates for observations at the end of Phase I, and the initial condition for Phase III was set to the predicted concentrations at eleven weeks of Phase II, which closely matched observations.

Table 1 Effective diffusion coefficients for sulfate. Extrapolated from effective bromide (non-reactive) diffusion quantified during Phase II using temperature and molecular-weight dependence.

	Cold diffusion in water [$\times 10^{-6}$ cm ² /s]	Warm diffusion in water [$\times 10^{-6}$ cm ² /s]
Bromide	15.0	20.9
Sulfate	7.5	10.6

$$\text{PDE: } \frac{dC}{dt} = \frac{d}{dx} \left(D \frac{dC}{dx} \right) - u \frac{dC}{dx} - kC$$

$$\begin{aligned} \text{BC \& IC: } & C(x=0, t) = C_0 \\ & \frac{dC(x=L, t)}{dx} = 0 \\ & C(x, t=0) = f(x) \end{aligned}$$

Direct solution, central differencing:

$$\frac{C_i^{n+1} - C_i^n}{\Delta t} = D_i \frac{(C_{i-1}^n - 2C_i^n + C_{i+1}^n)}{\Delta x^2} - u_i \frac{(C_{i-1}^n - C_{i+1}^n)}{2\Delta x} - kC_i^n$$

Discretized PDE:

$$C_i^{n+1} = C_{i-1}^n \left(D_i \frac{\Delta t}{\Delta x^2} - u_i \frac{\Delta t}{2\Delta x} \right) + C_i^n \left(1 - 2D_i \frac{\Delta t}{\Delta x^2} - k\Delta t \right) + C_{i+1}^n \left(D_i \frac{\Delta t}{\Delta x^2} + u_i \frac{\Delta t}{2\Delta x} \right)$$

Discretized BC & IC:

$$C_0 = C_0$$

$$C_L^{n+1} = C_{L-1}^n \left(2D_i \frac{\Delta t}{\Delta x^2} \right) + C_L^n \left(1 - 2D_i \frac{\Delta t}{\Delta x^2} - k\Delta t \right)$$

Table 2 boundary and initial conditions for model simulations. Velocity = 0 for all simulations.

Simulation	Boundary condition – Concentration at x = 0	Initial Condition – Concentration at t = 0
Warm sulfate – Loading North Bay	$C(x=0,t) = 283 \text{ mg/L}$	$C(x,t=0) = 34e^{\sqrt{\frac{0.35}{0.917}}(x)}$
Cold sulfate – Loading North Bay	$C(x=0,t) = 269 \text{ mg/L}$	$C(x,t=0) = 27e^{\sqrt{\frac{0.043}{0.65}}(x)}$
Warm sulfate – Loading Partridge	$C(x=0,t) = 395 \text{ mg/L}$	$C(x,t=0) = 84e^{\sqrt{\frac{0.35}{0.917}}(x)}$
Cold sulfate – Loading Partridge	$C(x=0,t) = 282 \text{ mg/L}$	$C(x,t=0) = 100$
Warm sulfate – Recovery	$C(x=0,t) = 37 \text{ mg/L}$ (North Bay); 116 (Partridge)	$C(x,t=0) = C(\text{end of warmloading})$
Cold sulfate – Recovery	$C(x=0,t) = 38 \text{ mg/L}$ (North Bay); 27 (Partridge)	$C(x,t=0) = C(\text{end of coldloading})$